

GEND

LOAN COPY

THIS REPORT MAY BE RECALLED
BY THE COUNTY CLERK
BY THE COUNTY CLERK

THE TECHNICAL LIBRARY

R. Kohli
R. S. Denning
M. P. Failey
D. W. Akers

Prepared for the
U.S. Department of Energy
Three Mile Island Operations Office
Internal Control No. DE-EC07-74D01570

[illegible]

DISCLAIMER

This book was prepared as an account of work sponsored by an agency of the United States Government. Neither the United States Government nor any agency thereof, nor any of their employees, makes any warranty, express or implied, or assumes any legal liability or responsibility for the accuracy, completeness, or usefulness of any information, apparatus, product or process disclosed, or represents that its use would not infringe privately owned rights. References herein to any specific commercial product, process, or service by trade name, trademark, manufacturer, or otherwise, does not necessarily constitute or imply its endorsement, recommendation, or favoring by the United States Government or any agency thereof. The views and opinions of authors expressed herein do not necessarily state or reflect those of the United States Government or any agency thereof.

**TMI-2 RCS MANWAY COVER BACKING PLATES
SURFACE DEPOSIT EXAMINATIONS**

**R. Kohl
R. S. Denning
M. P. Failey
D. W. Akers**

September 1987

**Battelle Columbus Division
505 King Avenue
Columbus, Ohio 43201**

**Prepared for EG&G Idaho, Inc.
Under Subcontract No. C86-130969
and the U.S. Department of Energy
Three Mile Island Operations Office
Under DOE Contract No. DE-AC07-76ID001570**

ABSTRACT

The surface deposits on the manway cover backing plates from steam generators A and B and from the pressurizer of the TMI-2 reactor were characterized to determine the concentration and distribution of the chemical elements and the radionuclides. This was accomplished by nondestructive (gamma scanning and autoradiography) and destructive (chemical, radiochemical, and microscopic analysis) examinations of the plates. The examination data were analyzed in terms of TMI-2 reactor accident information. The results showed that very small quantities of core materials and/or fission products were contained in the plate deposits. These quantities represent small fractions of the fission products/core materials released during the accident, with the possible exception of tellurium and silver, which could have implications regarding the form of transport of these materials.

SUMMARY

The manway cover backing (MCB) plates from steam generators A and B and the pressurizer from the TMI-2 reactor were examined at Battelle's Hot Cell Facility. The primary objective of the examination was to determine the abundance and distribution of core materials and/or fission products observed on the surface of the plates. The results were analyzed in terms of TMI-2 accident information.

Examinations conducted on the MCB plates included detailed chemical and radiochemical analyses and microscopy using a variety of analytical techniques. Results of these examinations and the conclusions derived are:

- Visual examination of the plates showed gray or white patchy deposits on the surface.
- Gamma-activity scanning and autoradiography showed very low Cs-137 activity across the diameter of the plates. Significant activity was observed only at the edge of the plates.
- The radionuclide content of the deposits from Plates A and B was 10 to 100 times higher than from the Plate P deposits. Also, the Cs-134/Cs-137 ratios were higher for P deposits, suggesting that the pressurizer Cs originated from a region of higher fuel burnup.
- Elemental analyses of the dissolved deposits gave relatively high values for Te, Ag, and Cd. This suggests that the release of these elements from the core was high and that they were transported a considerable distance before depositing.
- Metallographic examination of the plate samples showed the thickness of the surface deposits varied from 4-12 μm (Plates B and P) to 2-4 μm (Plate A). The deposits consisted mainly of Fe, Cr, and Ni, although evidence of In and Sn was also found.

- The MCB plate examinations indicate that, except for tellurium, only small fractions of the fission products, released from the fuel during the accident, deposited in the pressurizer and the steam generators. It should be recognized that higher amounts could have been deposited during the accident and subsequently washed from the surfaces.

ACKNOWLEDGMENTS

This report was prepared by Battelle Columbus Division (BCD) for EG&G Idaho, Inc. (EG&G) as an account of work sponsored by the United States Department of Energy (DOE). The authors are grateful to M. L. Russell and B. F. Saffell for useful discussions during the course of the project. They would like to thank Larry Kardos, Phil Schumacher, Andy Skidmore, Paul Tomlin, Paul Faust, and Tom Beddick for performance of the experimental work, and Marlene Linton, Rhoda McKenzie, and Darold Conrad for assistance with manuscript preparation. The project was supported by the U.S. Department of Energy under Subcontract No. C86-130969.

CONTENTS

| | |
|---|-----|
| ABSTRACT | 11 |
| SUMMARY | 111 |
| ACKNOWLEDGMENTS | v |
| CONTENTS | vi |
| 1. INTRODUCTION | 1 |
| 1.1 Background | 1 |
| 1.2 Manway Cover Backing Plate History | 4 |
| 1.2.1 RCS Description | 4 |
| 1.2.2 Manway Cover Backing Plate Description | 6 |
| 1.2.3 TMI-2 Accident and Recovery Period Environment | 6 |
| 2. EXAMINATION AND RESULTS | 13 |
| 2.1 Sample Receipt and Initial Inspection | 13 |
| 2.2 Visual Examination | 13 |
| 2.3 Total Radioactivity and Distribution | 20 |
| 2.3.1 Gamma-Ray Scanning | 20 |
| 2.3.2 Autoradiography | 25 |
| 2.4 Marking and Sectioning | 25 |
| 2.4.1 Sample Selection | 25 |
| 2.4.2 Preparation of Samples for Analysis | 29 |
| 2.5 Fission Product Abundance and Distribution Analysis Results | 35 |
| 2.6 Core Material Abundance and Distribution | 35 |
| 2.6.1 Inductively Coupled Argon Plasma Spectroscopy and Atomic Absorption Spectroscopy Analysis | 36 |
| 2.6.2 Spark Source Mass Spectrometric Analysis | 36 |
| 2.6.3 Metallography | 36 |
| 2.6.4 Scanning Electron Microscopy | 47 |

| | | |
|-----|--|----|
| 3. | TMI-2 ACCIDENT SCENARIO | 57 |
| 3.1 | Data Evaluation and Analysis Including Fission Product Inventory Estimation | 58 |
| 3.2 | Interpretation of the Results | 62 |
| 4. | REFERENCES | 63 |

FIGURES

| | | |
|-----|--|----|
| 1. | TMI-2 reactor coolant system piping and components | 5 |
| 2. | TMI-2 steam generator diagram | 7 |
| 3. | TMI-2 pressurizer layout | 8 |
| 4. | Video still-image views of TMI-2 steam generator tube sheet tops in March 1986 | 12 |
| 5. | Schematic of the shielded container showing the manway cover | 14 |
| 6. | Orientations of quadrants and directions with respect to surface X and the ID numbers on the TMI-2 plates | 15 |
| 7. | View of active surface of plate A | 16 |
| 8. | View of active surface of plate B | 17 |
| 9. | View of active surface of plate P | 18 |
| 10. | Cs-137 activity profile from the active surface X of manway cover plate A (scan direction is 3-1) | 21 |
| 11. | Cs-137 activity profile from the active surface X of manway cover plate A (scan direction is 4-2) | 22 |
| 12. | Cs-137 activity profile from the active surface X of manway cover plate B (scan direction is 1-3) | 23 |
| 13. | Cs-137 activity profile from the active surface X of manway cover plate P (scan direction is 4-2) | 24 |
| 14. | Autoradiograph of plate A | 26 |
| 15. | Autoradiograph of plate B | 27 |
| 16. | Autoradiograph of plate P | 28 |

| | |
|--|--------|
| 17. Sectioning plan for MCB plates | 30 |
| 18. Sectioning plan for MCB plate samples for chemical analyses and metallography | 31 |
| 19. Schematic of I-129 volatilizing and trapping apparatus | 32 |
| 20. Optical micrographs of specimens from plate A | 41, 42 |
| 21. Optical micrographs of specimens from plate B | 43, 44 |
| 22. Optical micrographs of specimens from plate P | 45, 46 |
| 23: SEM photographs of specimen A1 | 48 |
| EDS spectrum of surface deposit from specimen A1 | 49 |
| 24: SEM photograph of specimen B4 | 50 |
| EDS spectrum of surface deposit from specimen B4 | 51 |
| 25: SEM photograph of specimen P1 | 52 |
| EDS spectrum of surface deposit from specimen P1 | 53 |
| 26: SEM photographs of specimen A4 | 54 |
| EDS spectrum of surface deposit from specimen A4 | 55 |
| WDS spectrum of surface deposit from specimen A4 | 56 |

TABLES

| | |
|---|----|
| 1. Surface contamination and radiation readings measured on the MCB plates | 19 |
| 2. Location and identification of samples obtained after sectioning of the MCB plates | 33 |
| 3. MCB plate sample radionuclide content | 35 |
| 4. MCB plate samples elemental surface concentrations | 37 |
| 5. Mass spectrometric analysis of MCB plate samples | 38 |
| 6. Measured surface deposition and core inventory fractions of radionuclides deposited on the MCB plates | 59 |

TMI-2 RCS MANWAY COVER BACKING PLATES
SURFACE DEPOSIT EXAMINATIONS

1. INTRODUCTION

One of the major objectives of the technical data acquisition program for the Three Mile Island Unit 2 (TMI-2) reactor is to provide information on the release, transport, and deposition of fission products and other radionuclides during severe core-damage accidents. Some of this information is being obtained by detailed characterization of deposits on surfaces within the TMI-2 reactor coolant system.

This report describes the nondestructive and destructive examinations conducted on the manway cover backing plates from steam generators A and B and the pressurizer from the TMI-2 reactor. The manway cover backing (MCB) plates from the steam generators and the pressurizer are components sufficiently removed from the reactor core to provide representative locations for transport and deposition of core materials. The results of these examinations are interpreted in terms of TMI-2 accident information.

1.1 Background

The examination of surface deposits on the manway cover backing plates from the TMI-2 pressurizer and steam generator upper head is a small part of a large and complex TMI-2 Accident Evaluation Program Sample Acquisition and Examination Plan.¹

Although the March 28, 1979, accident at TMI-2 involved severe damage to the core of the reactor, it had no observable effects on the health and safety of the public in the area. That such a severe core-disruption accident would have no consequent health or safety effects has resulted in the questioning of earlier light water reactor (LWR) safety studies and estimates. In an effort to resolve these questions, several major research programs have been initiated by a variety of organizations concerned with nuclear power plant safety. The U.S. Nuclear Regulatory Commission (NRC) has embarked on a thorough review of reactor safety issues, particularly

the causes and effects of core-damage accidents. Industrial organizations have conducted the Industry Degraded Core Rulemaking (IDCOR) Program. The U.S. Department of Energy (DOE) has established the TMI-2 Program to develop technology for recovery from a serious reactor accident and to conduct relevant research and development that will substantially enhance nuclear power plant safety.

Immediately after the TMI-2 accident, four organizations with interests in both plant recovery and accident data acquisition formally agreed to cooperate in these areas. These organizations, commonly referred to as the GEND Group--GPU Nuclear Corporation, Electric Power Research Institute, Nuclear Regulatory Commission, and Department of Energy--are actively involved in reactor recovery and accident research. At present, DOE is providing a portion of the funds for reactor recovery (in those areas where accident recovery knowledge will be of generic benefit to the U.S. LWR industry) as well as the preponderance of funds for severe accident technical data acquisition (such as the examination of the damaged core).

This work by Battelle Columbus Division is part of the DOE program to involve private laboratories in the United States in the TMI-2 Accident Evaluation Program that is coordinated by EG&G Idaho, Inc. (EG&G). The EG&G involvement with the TMI-2 accident has been continuous, initially providing technical support and consultation from the Idaho National Engineering Laboratory (INEL). In 1979, EG&G received an assignment from DOE to collect, analyze, distribute, and preserve significant technical information available from TMI-2. This assignment was expanded (in 1981 and 1984) to include: (a) conducting research and development activities intended to effectively exploit the generic research and development challenges at TMI-2, and (b) developing an understanding of the accident sequence of events in the area of core damage and behavior of core radionuclides (fission products) and materials. The TMI-2 Accident Evaluation Program report² defines the program required to implement the DOE assignments and contains the guidelines and requirements for TMI-2 sample acquisition and examinations.

The already-completed portion of the Sample Acquisition and Evaluation (SA&E) Plan includes in situ measurements and sample acquisition and examinations involving private organizations and state and federal agencies. It has provided the postaccident core and fission product end-state data that indicate the following:

- The current estimate of damage and reconfiguration of the core is as follows:

| Core Region | Core Material (%) |
|--|-------------------|
| Still standing rod bundle geometry | 42 |
| Loose debris (unmelted and previously molten core material mixture) below the cavity in the upper core region (the cavity was 26% of the original core volume) | 25 |
| Previously molten core material: | 33: |
| Retained in core boundary | 20 |
| Escaped from core boundary | 13 |

- Some uranium dioxide fuel melting occurred with temperatures up to at least 3100 K.
- Between 10 and 20 metric tons of core and structural materials relocated into the space between the reactor vessel bottom head and the elliptical flow distributor.
- Significant fission product retention was by the core materials inside the reactor vessel and by reactor coolant system water and reactor building basement water and concrete outside the reactor vessel.

The pressurizer and steam generator manway cover backing plate surface deposit examinations are part of the Reactor Coolant System Fission Product Inventory (RCS FPI) portion of the TMI-2 Accident Evaluation Program SA&E Plan. This part of the plan also includes examination of loose deposits from reactor coolant system horizontal and low-point surfaces, in situ

video and boroscope surveys of the reactor coolant system vessels, and piping for locating core material deposits and in situ gamma spectrometer surveys for locating uranium in the reactor coolant system. The TMI-2 AEP requirements and/or objective for the RCS FPI Sample Acquisition and Examination Program are:

"All present experience in characterizing the plant indicates relatively small fission product deposition on the reactor system surfaces external to the reactor vessel. However, the primary cooling system surface deposition may provide the only benchmark for the fission product transport during the core degradation phase of the accident. In particular, the retained fission product chemical forms may be related to the fission product chemistry during the transient and the reactor vessel chemical environment during the accident. Analysis of the core material debris deposited in the RCS will be conducted to enhance our understanding of the plant hydraulic conditions during or shortly after the accident."²

"For each sample, the following characteristics should be determined:

- Physical appearance,
- Elemental and chemical composition,
- Particle size distributions, density, and surface texture, and
- Radiochemical measurements of retained fission product concentrations and chemical forms."²

1.2 Manway Cover Backing Plate History

1.2.1 RCS Description

TMI-2 reactor coolant system piping and components are shown in Figure 1 and include the following:

- o A reactor vessel containing the uranium-fueled core.

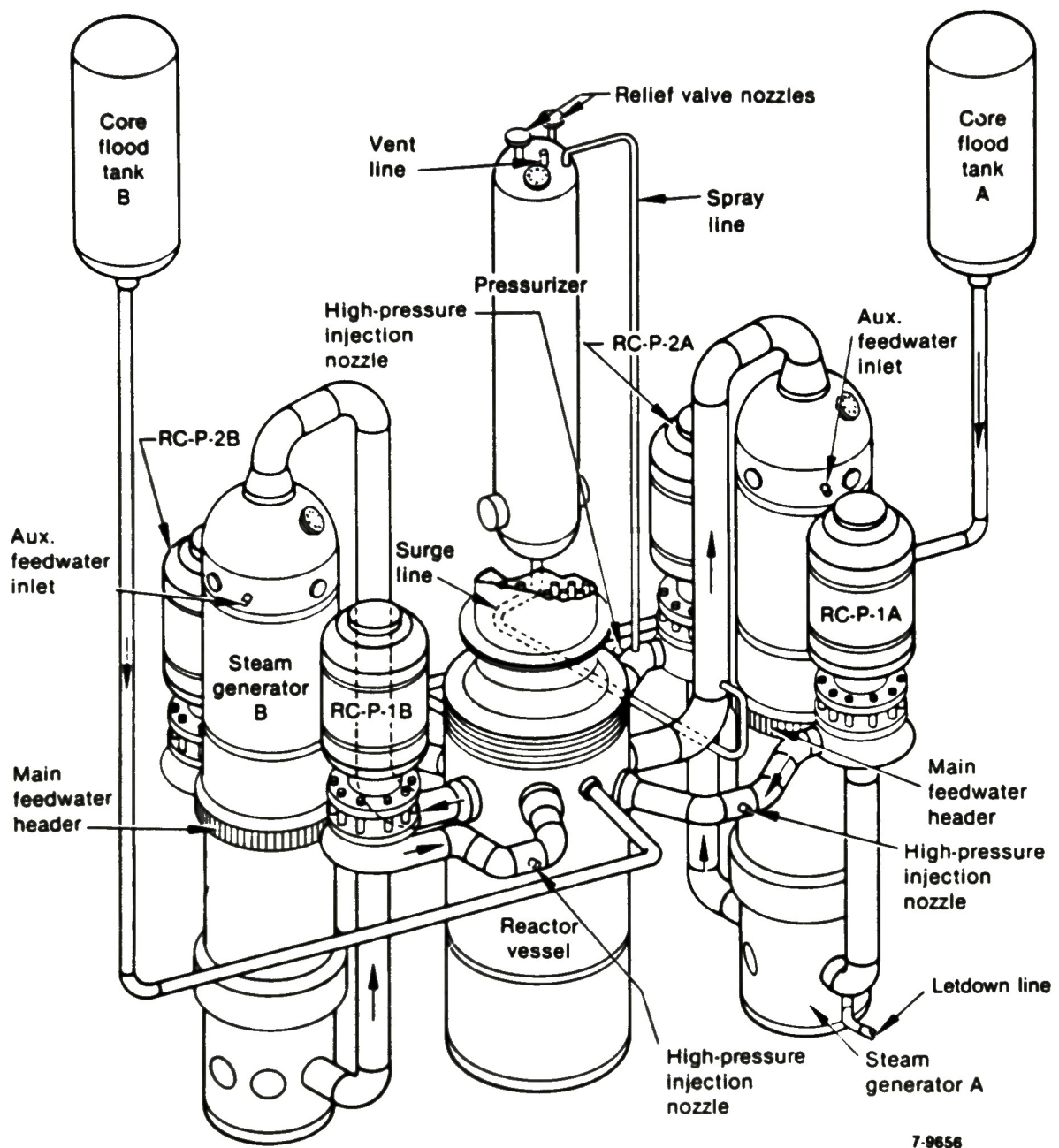


Figure 1. TMI-2 reactor coolant system piping and components.

- Dual reactor cooling loops (A and B) consisting of the candy-cane-shaped hot legs from the reactor vessel upper plenum to the steam generator tops, two single-pass type steam generators (Figure 2), dual (four total) cold legs from the steam generator bottom back to the reactor vessel via the four reactor coolant pumps.
- A pressurizer (Figure 3) connected to the cooling loops by a surge line from the A-loop hot leg to the pressurizer bottom and a spray line from the A-loop cold leg (downstream of pump RC-P-2A) to the pressurizer top.
- Dual core flood tanks connected to the reactor vessel.

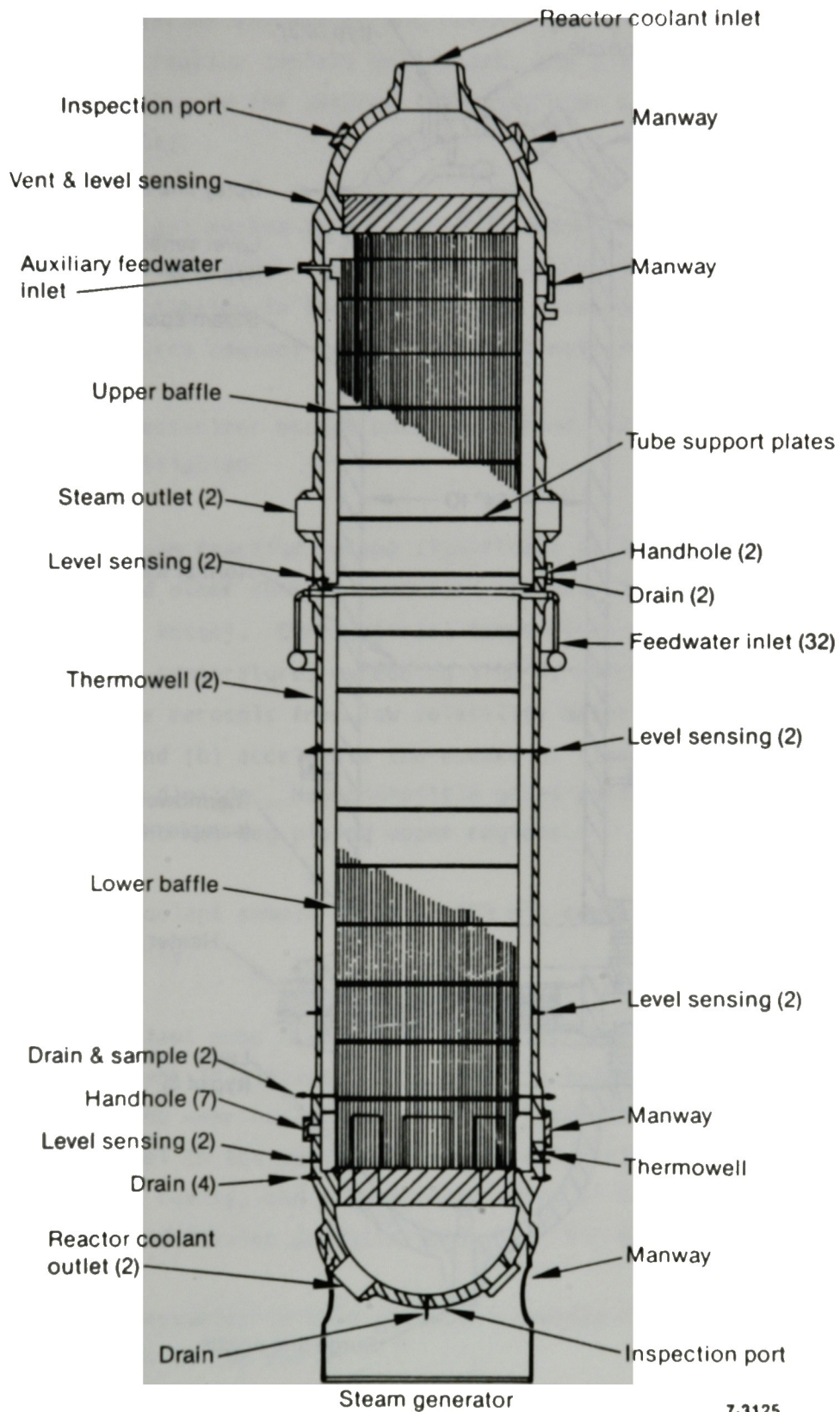
1.2.2 Manway Cover Backing Plate Description

The manway cover backing plates are 3/4-in.-thick, Type 304 stainless steel discs used to protect the carbon steel manway covers from the reactor coolant in the upper head regions of the pressurizer and steam generators (see Figures 2 and 3). The backing plate inner surfaces that were exposed to the reactor coolant are approximately 16-in. in dia.

1.2.3 TMI-2 Accident and Recovery Period Environment

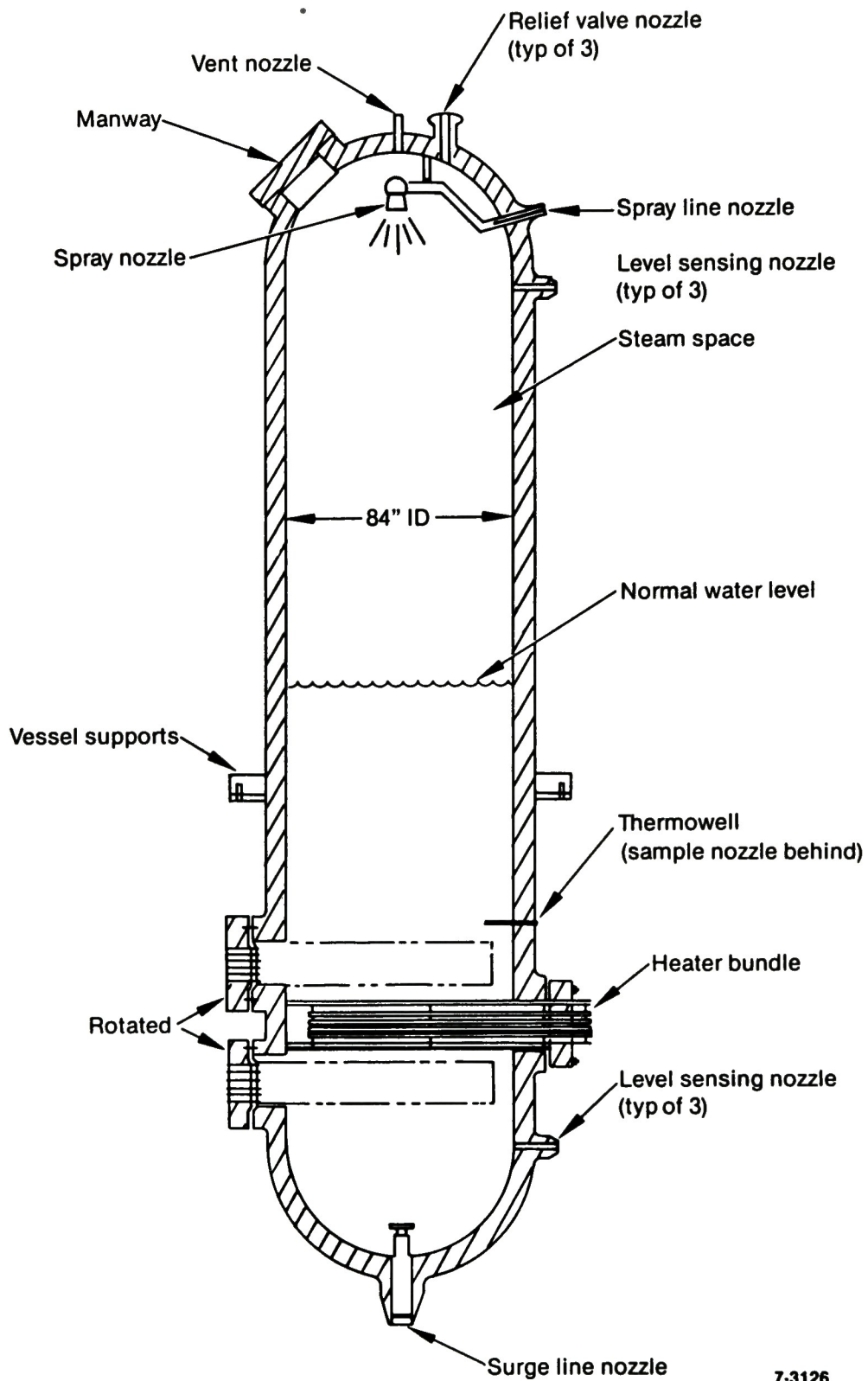
During and after the TMI-2 accident sequence that lasted until natural circulation cooling commenced (approximately 30 days after accident initiation), many events occurred that affected the character and distribution of core materials and fission products which escaped from the reactor vessel to the reactor coolant system. The most significant events include the following:

- Fission product and a small uranium fraction release commenced in the reactor vessel at approximately 138 min after accident initiation when fuel rod rupture commenced. Reactor coolant pump operation had ceased, and the available escape paths were (a) through the A-loop hot leg, surge line, and pressurizer



7-3125

Figure 2. TMI-2 steam generator diagram.



7-3126

Figure 3. TMI-2 pressurizer layout.

because the pilot-operated relief valve (PORV) was stuck open, releasing reactor coolant to the reactor building basement through the reactor coolant drain tank, and (b) through the A-loop cold leg to the letdown line (upstream of reactor coolant pump RCP-P-1A).

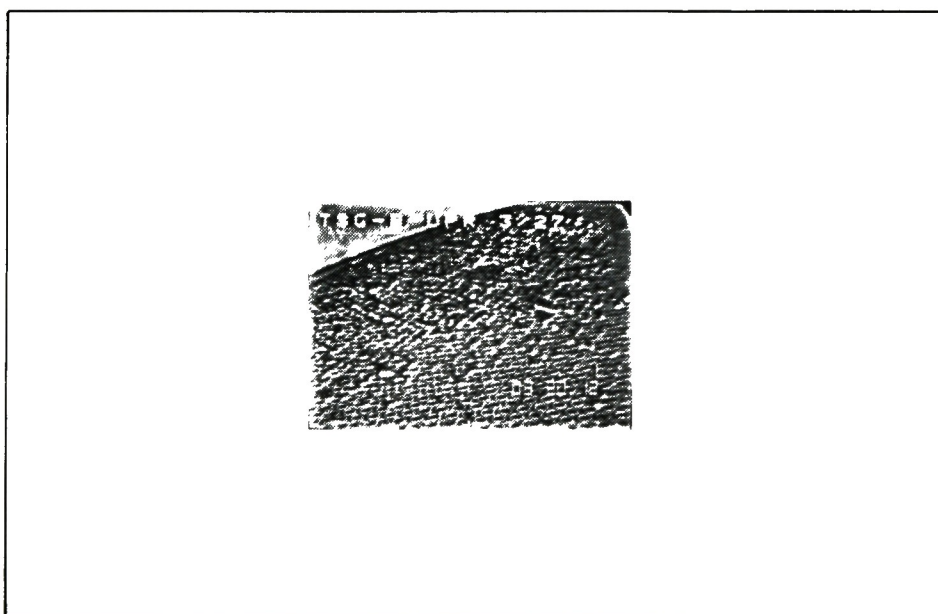
- Reactor coolant system temperatures exceeded the coolant saturation temperature from 136 min to approximately 16 h after accident initiation in the hot legs and occasionally in the cold legs. Measured coolant temperatures did not exceed 725 K.
- The PORV/pressurizer escape path was closed 142 min after accident initiation.
- Zircaloy-steam reaction became significant at 144 min, releasing hydrogen and other chemical reaction products into the coolant in the reactor vessel. Core material temperatures continued to rise and reached temperatures exceeding 3100 K, which could:
(a) generate aerosols from low volatility materials and chemical reactions and (b) accelerate the escape of fission products from the uranium dioxide. Noncondensable gases collected in the steam generator and hot leg piping upper regions.
- A reactor coolant sample taken at 163 min contained 140 $\mu\text{Ci/ml}$ gross activity.
- Reactor coolant pump RC-P-2B was energized from 174 to 192 min after accident initiation. This event is believed to have reflooded the over-heated core region, fragmenting most of the standing fuel in the upper core region and creating the upper core region cavity, and caused circulation of core material particles and fission products throughout the B-loop components.
- The PORV/pressurizer escape path was reopened from 192 to 197 min and from 220 to 318 min.

- At 227 min, a significant relocation of core material from the core region into the flooded reactor vessel lower plenum region occurred, which would likely increase the escape of core material and fission products to the letdown system escape path.
- A sustained high pressure injection period commenced at 267 min and continued to 544 min.
- A reactor coolant sample taken at 283 min contained >500 $\mu\text{Ci/ml}$ gross activity.
- The PORV/pressurizer escape path was cycled open repeatedly during the 340 to 458 min period to prevent RCS overpressurization and was also opened from 458 to 550, 565 to 589, 600 to 668, 756 to 767, and 772 to 780 min to depressurize the RCS for core flood injection.
- Core flood tank injection probably occurred from 511 to 550 min after accident initiation. This event is believed to have caused a back flow leak path to develop from the reactor coolant system to flood tank B due to incomplete check valve reseating.
- A reactor coolant system pressurization in the 840 to 900 min period probably forced coolant and core material aerosols and volatile fission products from the reactor vessel into flood tank B.
- Forced circulation cooling of the reactor was resumed at 949 min (15 h 49 min) through the A-loop with reactor coolant pump RC-P-1A. This action flushed the noncondensable gases from the A-loop steam generator and hot leg upper regions.
- Letdown flow was lost from 18 h 34 min to 26 h 30 min.

- A reactor coolant sample taken at 36 h and 15 min measured >1000 R/h on contact.
- At 6 days after accident initiation, the noncondensable gas bubble in the B-loop upper region appeared to be gone.
- Natural circulation cooling of the reactor commenced 30 days and 10 h after accident initiation using both coolant loops. Steam generator B was later isolated.
- Reactor coolant water cleanup using the SDS/EPICOR-II system commenced 2 years and 106 days (07/12/81) after accident initiation and included cleanup of an equivalent of four reactor coolant system volumes of reactor coolant water after the accident.
- Between the accident and the manway cover removal, the reactor coolant has been a water solution with the following target specifications.
 - ph: 7.5 to 7.7
 - boron: 5000 to 5350 ppm
 - buffer: NaOH
- The RCS liquid volume was drawn down for initial reactor disassembly in July 1982, uncovering the pressurizer and steam generator upper regions. Figure 4 shows video still-images of the conditions at the top of the steam generator tube sheet when the manway covers were removed in March 1986.
- GPUN removed surface deposit samples from the manway cover backing plates using scraping techniques after the plates were removed from the reactor coolant system. The results of the GPUN analysis of the surface deposit scrape samples are reported in References 3 and 4.



A-loop steam generator tube sheet top



B-loop steam generator tube sheet top

Figure 4. Video still-image views of TMI-2 steam generator tube sheet tops in March 1986.

2. EXAMINATION AND RESULTS

2.1 Sample Receipt and Initial Inspection

The MCB plates from steam generators A and B (designated Plate A and Plate B) and the pressurizer (Plate P) were received in separate shielded containers (Figure 5) on August 4, 1986, at the Battelle Hot Cell Facility in West Jefferson, Ohio. The plates were removed from the shielded containers and monitored for surface contamination and radiation readings. The results are given in Table 1.

Plates A and B had identification numbers stamped on surface Y, while the ID number on Plate P was scribed on that surface. These numbers were used for orientation purposes for all subsequent examinations of the plates. Figure 6 describes the exact Battelle orientations of each quadrant with respect to the active surface X on each of the three plates.

2.2 Visual Examination

Each plate was visually examined through the hot cell window. The surface features were documented by means of black and white photographs shown in Figures 7-9.

In general, the plates exhibited no unusual features on their surfaces. Plate P appeared to be covered by a uniform gray surface layer. Plate A, on the other hand, appeared to have only patchy white areas of surface deposits, while the surface of Plate B was smooth and shiny. This suggests that any previous deposits on Plate B must have been removed in the reactor. These observations are also consistent with the subsequent Cs-137 gamma scans of the plates.

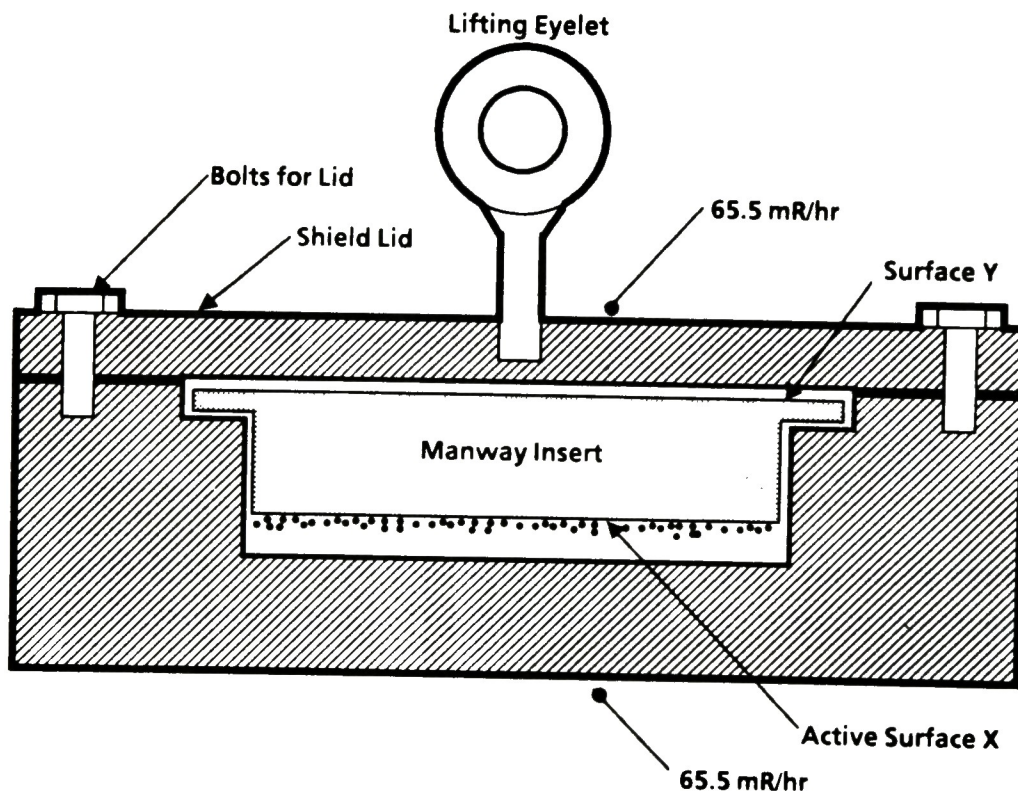


Figure 5. Schematic of the shielded container showing the manway cover.

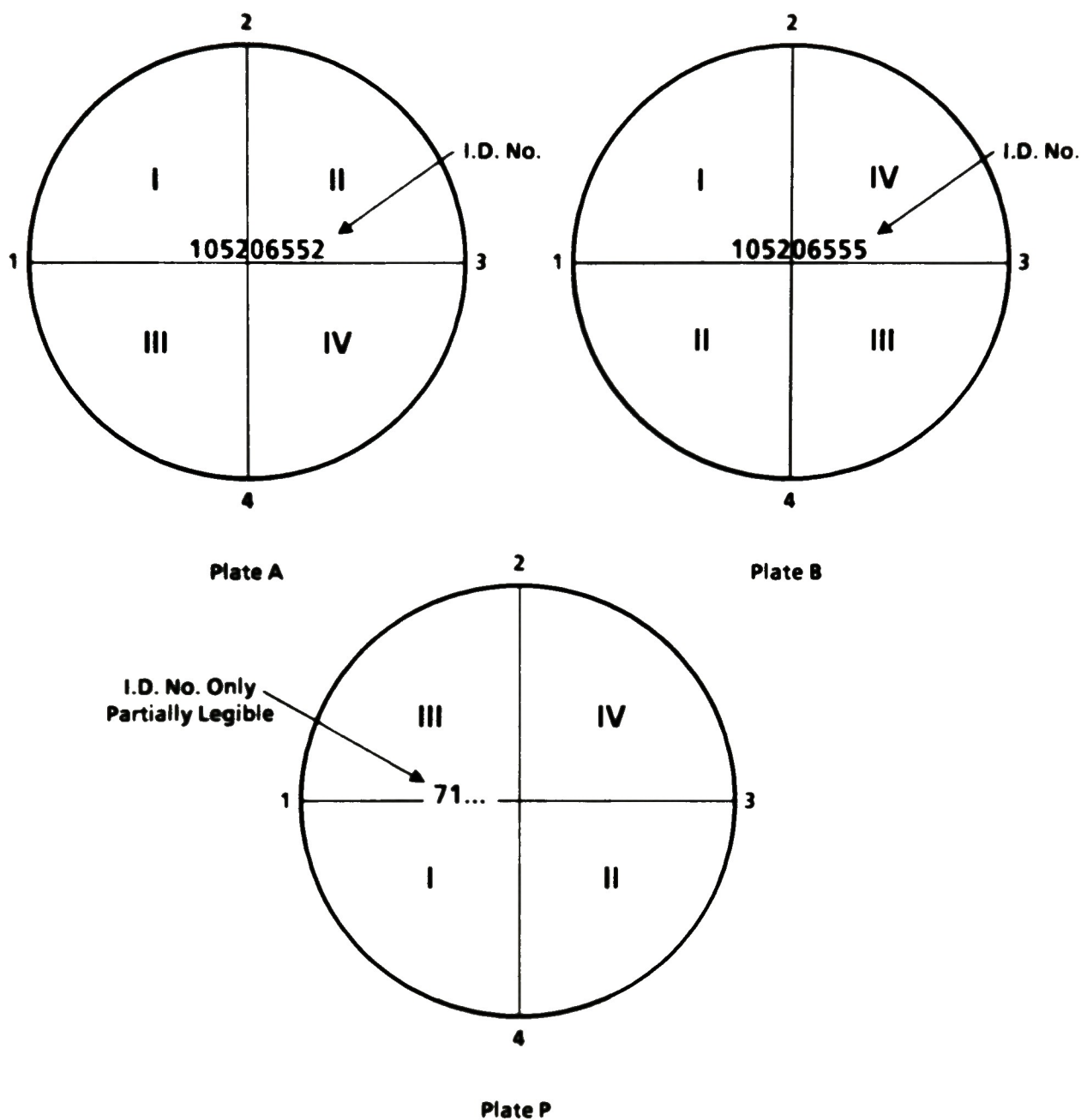


Figure 6. Orientations of quadrants and directions with respect to surface X and the ID numbers on the TMI-2 plates.

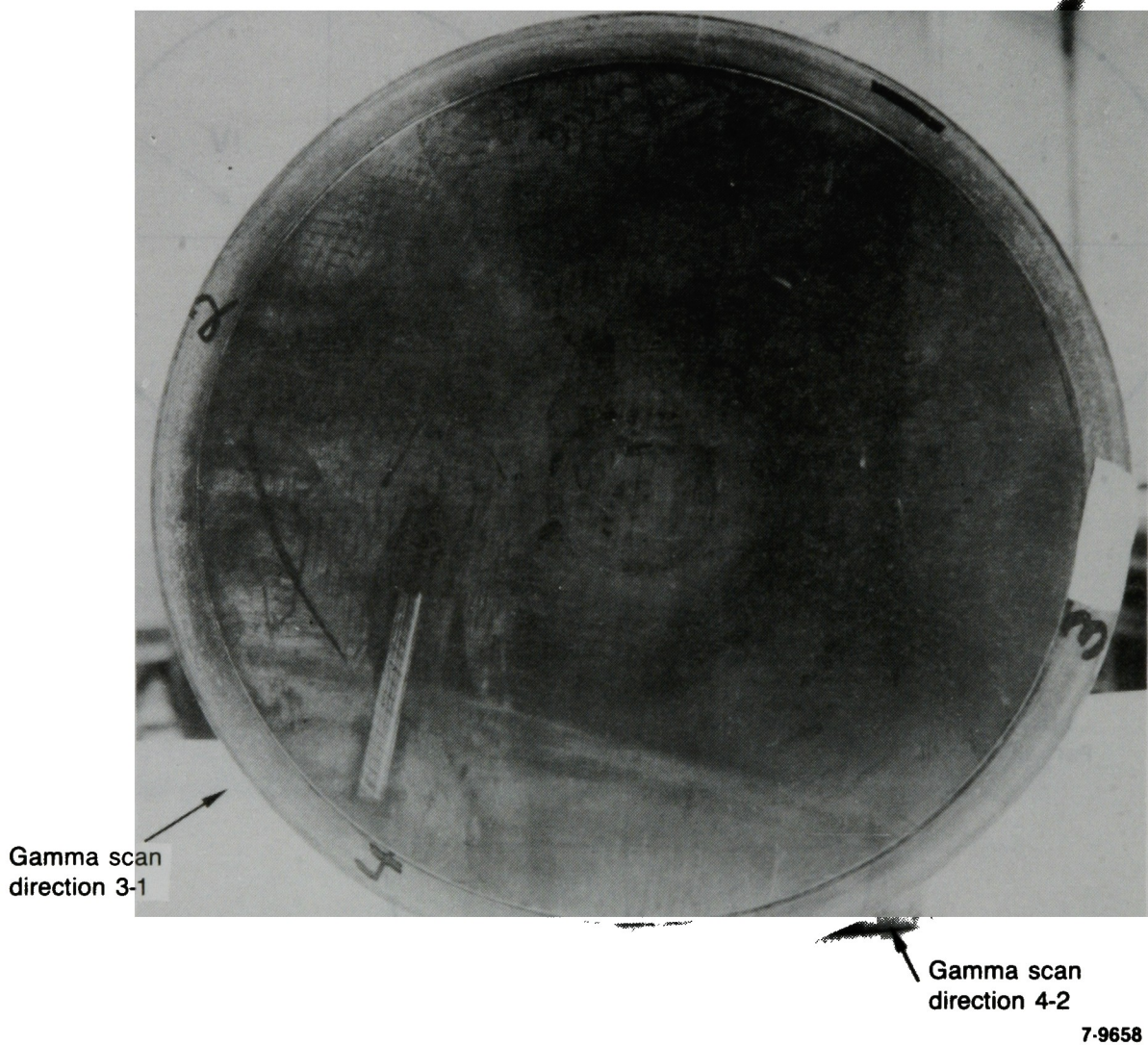
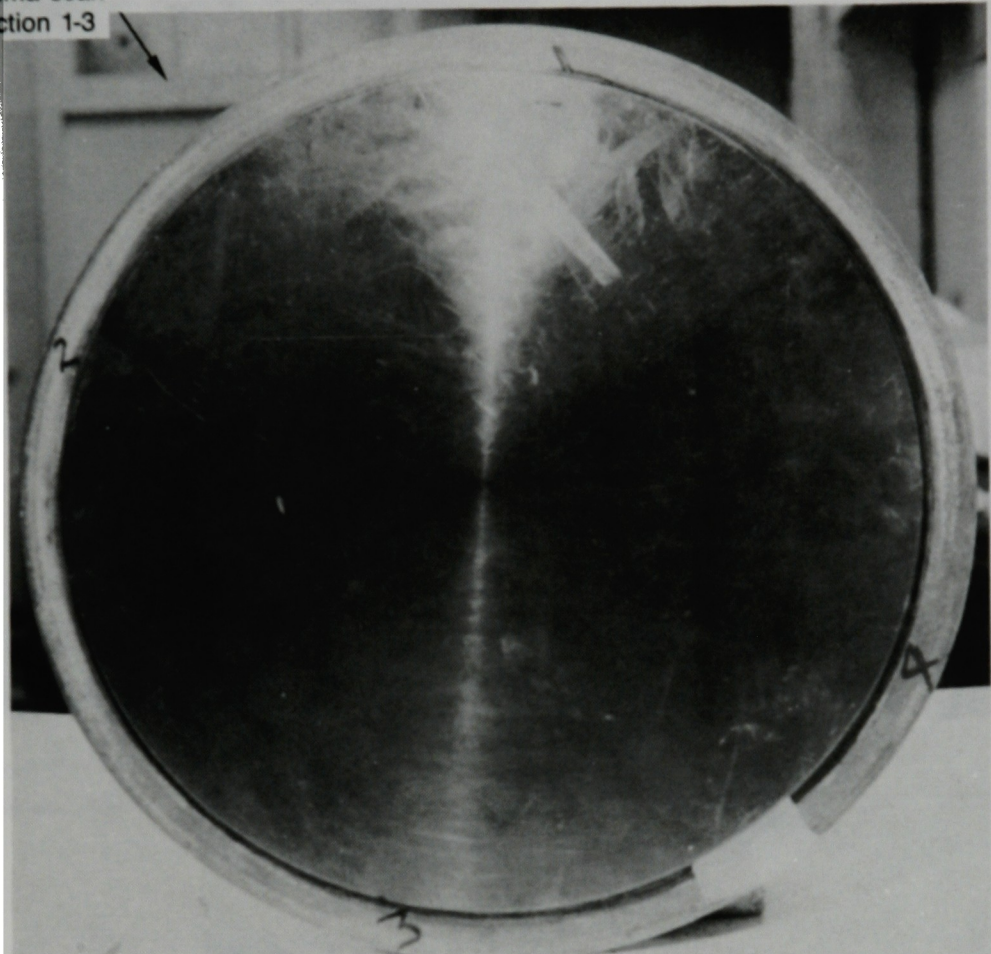


Figure 7. View of active surface of plate A.

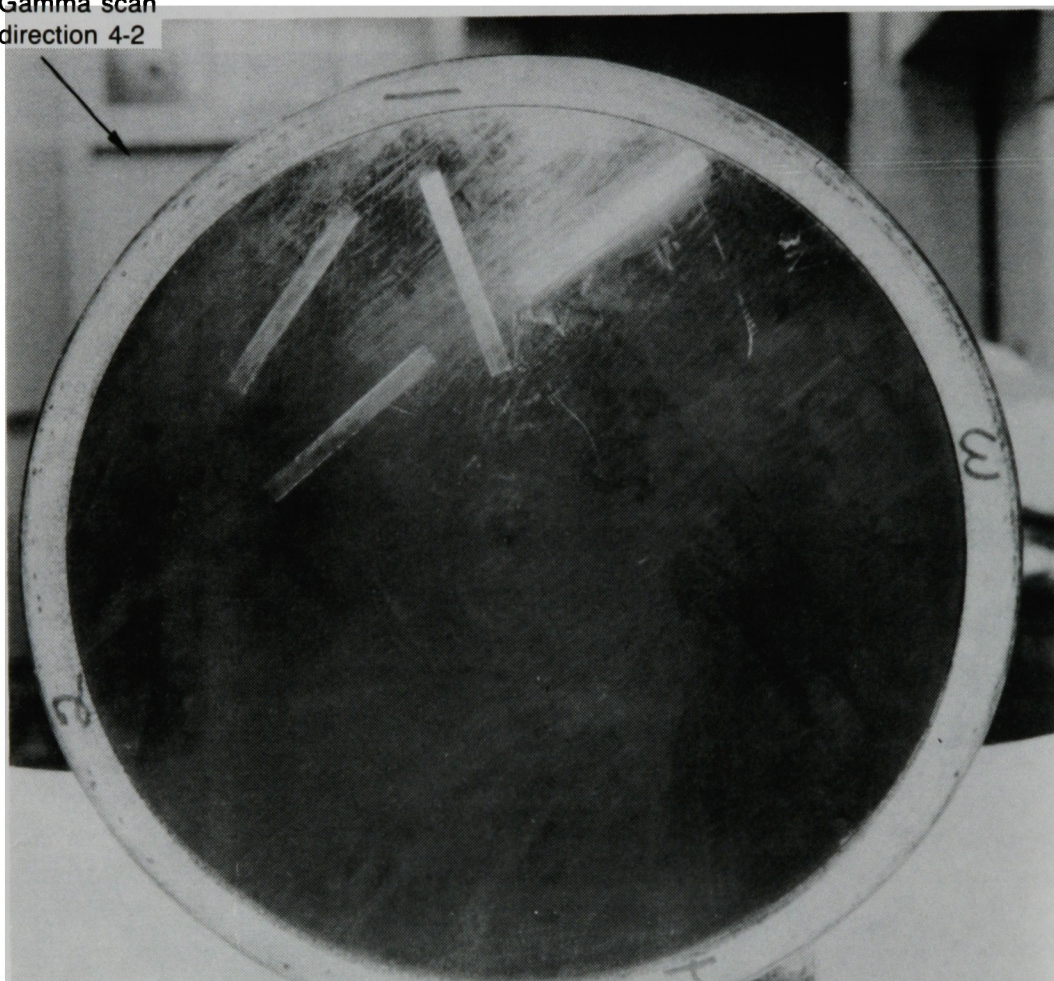
Gamma scan
Direction 1-3



7-9657

Figure 8. View of active surface of plate B.

Gamma scan
direction 4-2



7-9659

Figure 9. View of active surface of plate P.

TABLE 1. SURFACE CONTAMINATION AND RADIATION READINGS MEASURED ON THE MCB PLATES

| <u>Plate Identification</u> | <u>Surface^a</u> | <u>Smearable Activity^b</u> | <u>Radiation Reading^c</u> |
|-----------------------------|----------------------------|---------------------------------------|--------------------------------------|
| A | X (Active) | $>4 \times 10^6$ | 500 |
| | Y (Other) | $>2 \times 10^6$ | 300 |
| B | X (Active) | $>2 \times 10^6$ | 350 |
| | Y (Other) | $>1 \times 10^6$ | 200 |
| P | X (Active) | $>3 \times 10^6$ | 450 |
| | Y (Other) | $>1 \times 10^6$ | 300 |

a. See Figure 1 for location of these surfaces.

b. dpm/dm².

c. β - γ contact - activity, mR/hr.

2.3 Total Radioactivity and Distribution

2.3.1 Gamma-Ray Scanning

To determine if surface variation existed in the deposited radioactivity, each plate was gamma-ray scanned along one complete diameter. For this purpose, the Battelle West Drum Counting System (WDCS) was used. The WDCS employs an intrinsic germanium detector, coupled to a minicomputer-based multichannel analyzer, to obtain gamma-ray spectra of waste packages generated at the hot cell. The system collimation was modified so that small areas (~1.5 cm in dia) of the MCB plates could be scanned. The system has a drive mechanism that can translate the component to be scanned vertically past the detector, thereby allowing energy spectra to be obtained at various points along the direction of translation. By correcting the raw data for background radiation, the relative gamma-ray activities of the most abundant isotopes can be determined as a function of distance along the axis of translation of the plate.

Since the plates were highly contaminated, an aluminum box with a thin plexiglass window was fabricated to contain each plate during gamma-ray scanning. The box containing the plate was then mounted on the WDCS and scanned along the axis of interest by counting for 100 sec at 1 cm intervals. Because plate A was scanned first, two scans were performed along directions 3-1 and 4-2 (Figure 6) to determine if there are any major differences in the gamma activities between the two directions. The results are shown in Figures 10 and 11 which plot the relative Cs-137 activity as a function of distance from the edge of the plate. (Initial gamma scans had shown the surface activity to contain mainly Cs-137 with very minor amounts of Co-60 and Cs-134 present. Because of these small amounts of the latter isotopes, obtaining statistically significant Co-60 and Cs-134 counts would have required a prohibitively extended effort. Hence, all gamma scans are shown as Cs-137 activity profiles.) Inspection of these figures shows very little discernible difference between the activity profiles in the two scan directions. Hence, Plates B and P were scanned only along directions 1-3 and 4-2, respectively (see Figure 6). The results are shown in Figures 12 and 13. In comparing the results, the

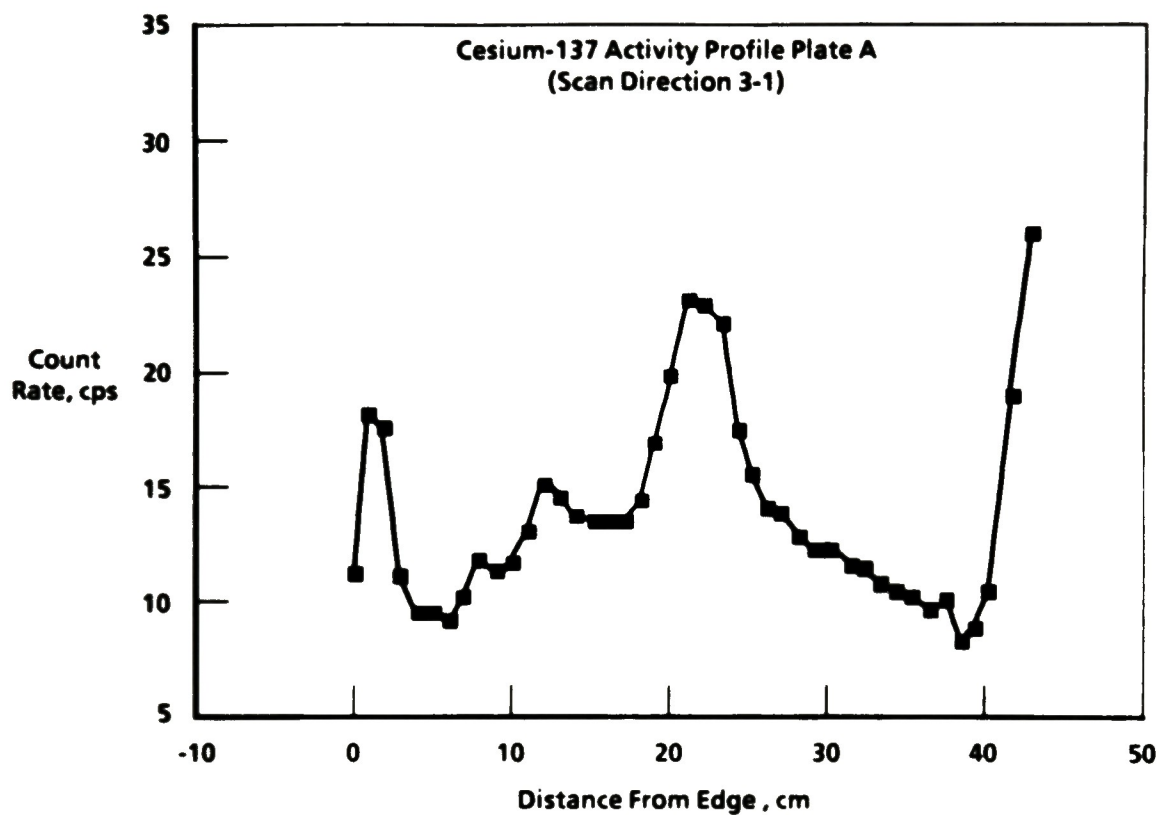


Figure 10. Cs-137 activity profile from the active surface X of manway cover plate A (scan direction is 3-1).

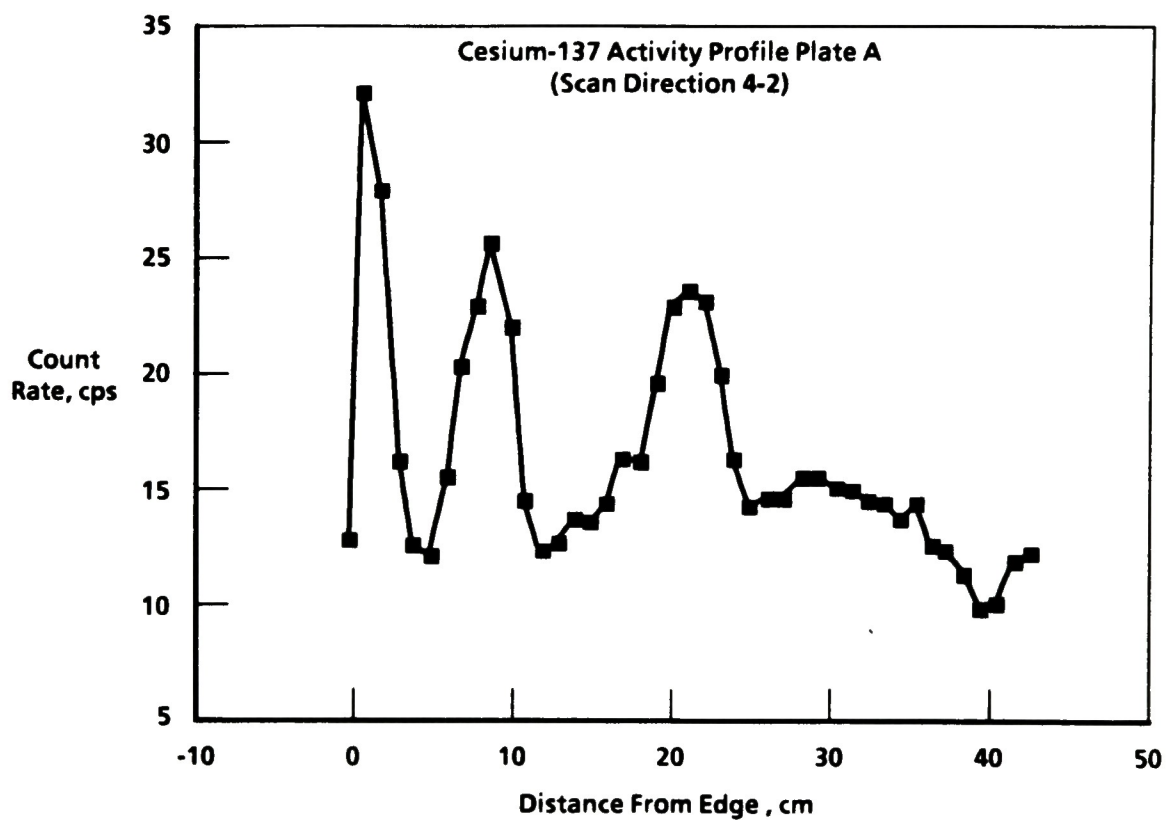


Figure 11. Cs-137 activity profile from the active surface X of manway cover plate A (scan direction is 4-2).

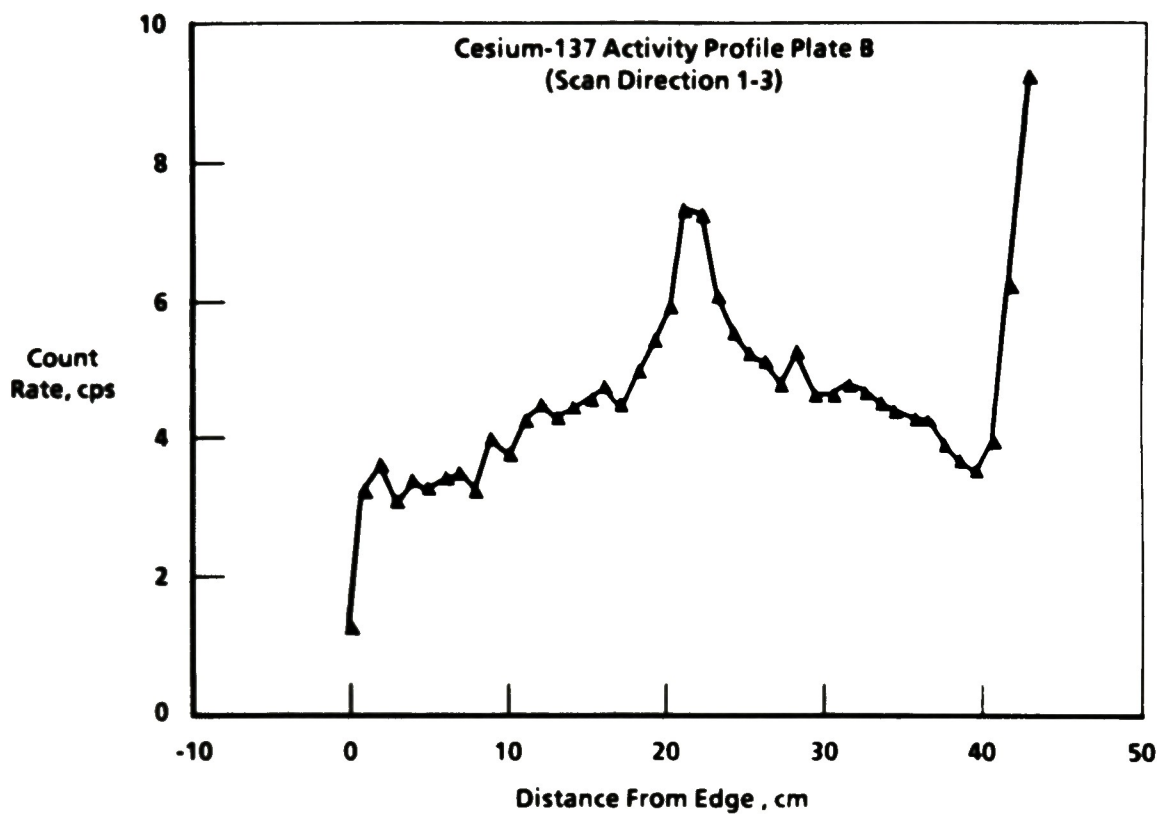


Figure 12. Cs-137 activity profile from the active surface X of manway cover plate B (scan direction is 1-3).

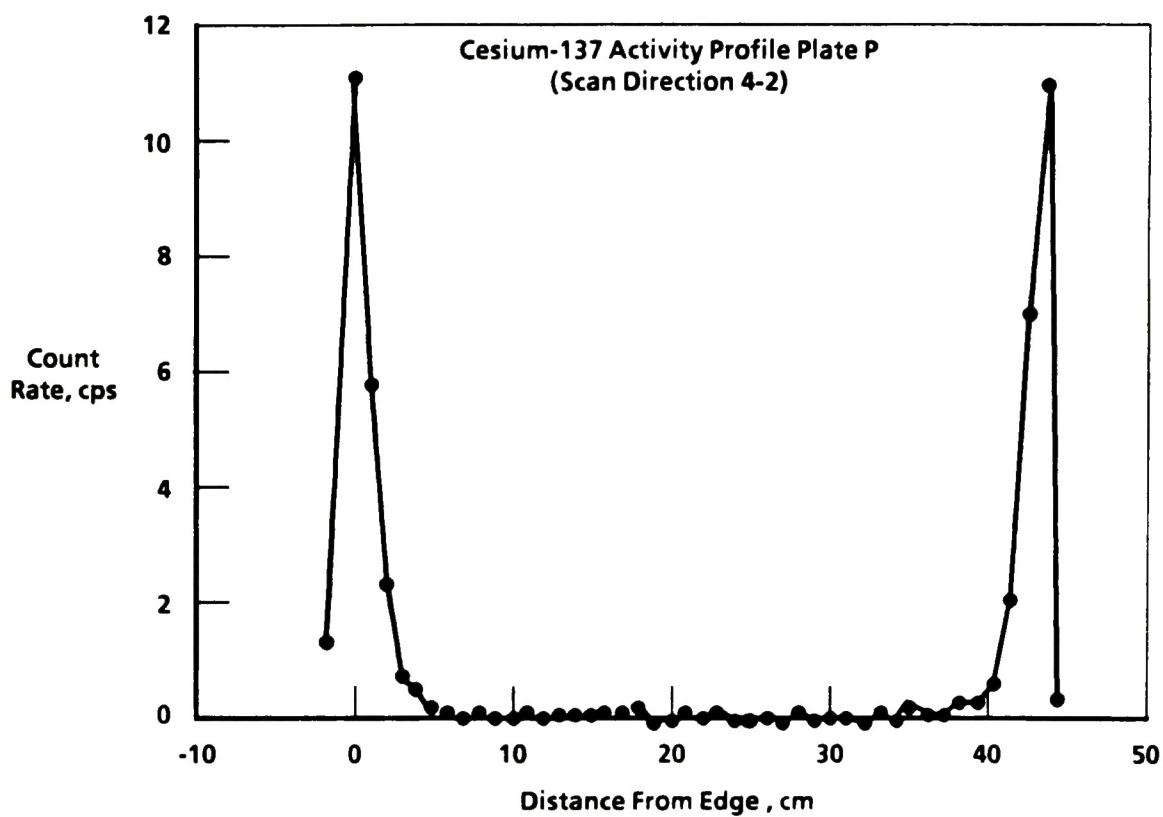


Figure 13. Cs-137 activity profile from the active surface X of manway cover plate P (scan direction is 4-2).

Cs-137 activity profiles show very low count rates, except near the edges of the plates. In fact, Plate P shows significant Cs-137 activity only within 1 cm of the edge; the activity profile goes to near zero across the remaining surface (Figure 12). Plate B, on the other hand, exhibits a Cs-137 profile very similar to that obtained on Plate A, although the overall count rate was approximately five times lower than on Plate A.

2.3.2 Autoradiography

To determine the distribution of gamma energy-emitting isotopes on the surface of the MCB plates, the plates were autoradiographed. Each plate was covered on its active surface with a thin (0.1 mm) polyethylene film to prevent contamination of the radiographic film holder. A 35 x 43 cm X-ray film was contained in the film holder, which was then placed in intimate contact with each plate and exposed for 45 seconds (Plate P) and 60 seconds (Plates A and B), respectively.

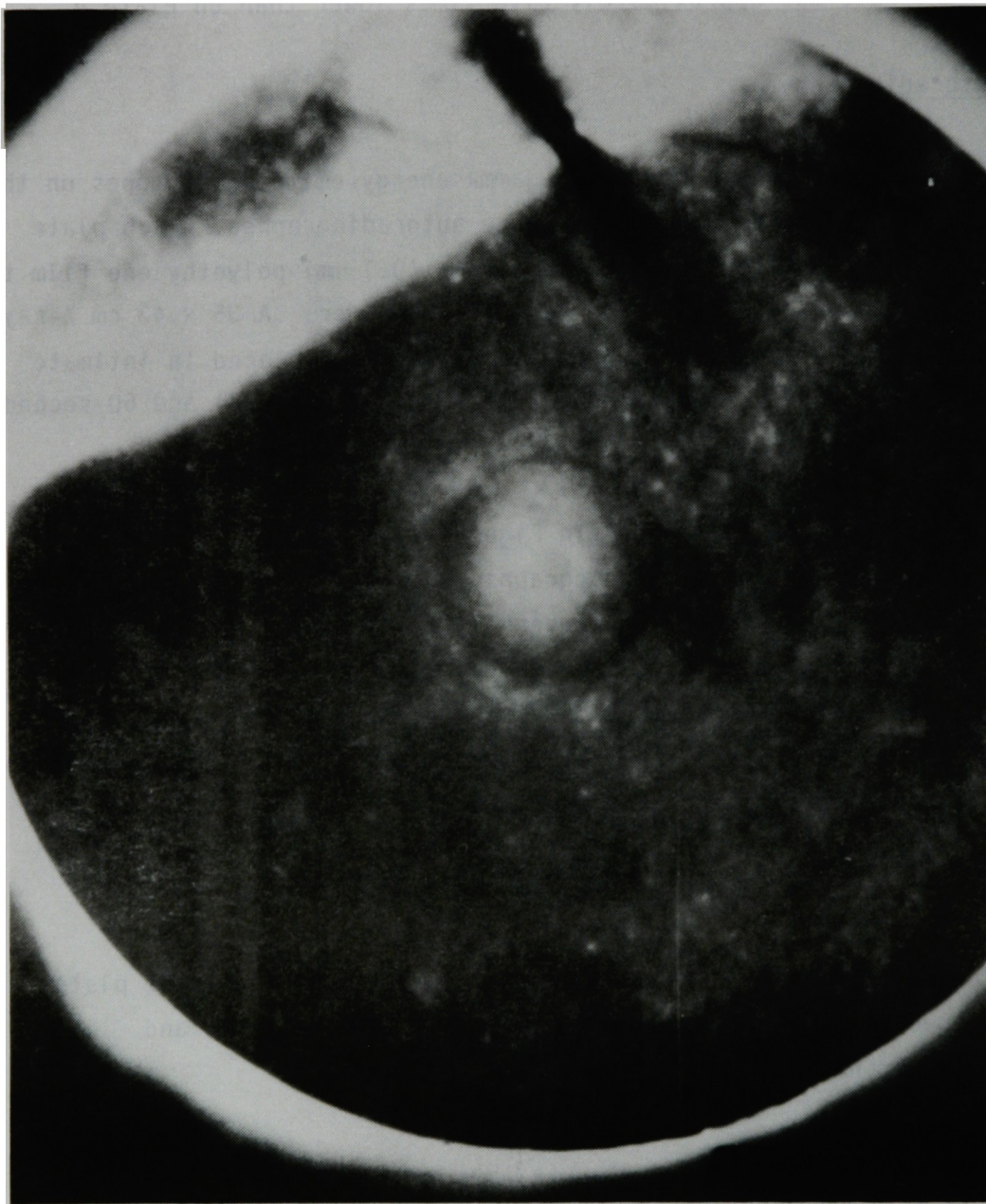
The autoradiographs are shown in Figures 14-16. Very little gamma activity is evident in the autoradiographs, which is not surprising since the gamma scans had previously shown very little activity on the surface of the plates. Closer inspection of the radiographs reveals that the gamma activity is uniformly distributed over the surface, in agreement with the results of the gamma scans. The Plate P radiograph shows significant gamma activity only at the very edges of the plate.

2.4 Marking and Sectioning

Following completion of the nondestructive examinations, the plates were sectioned to obtain samples for chemical, radiochemical, and microscopic examination.

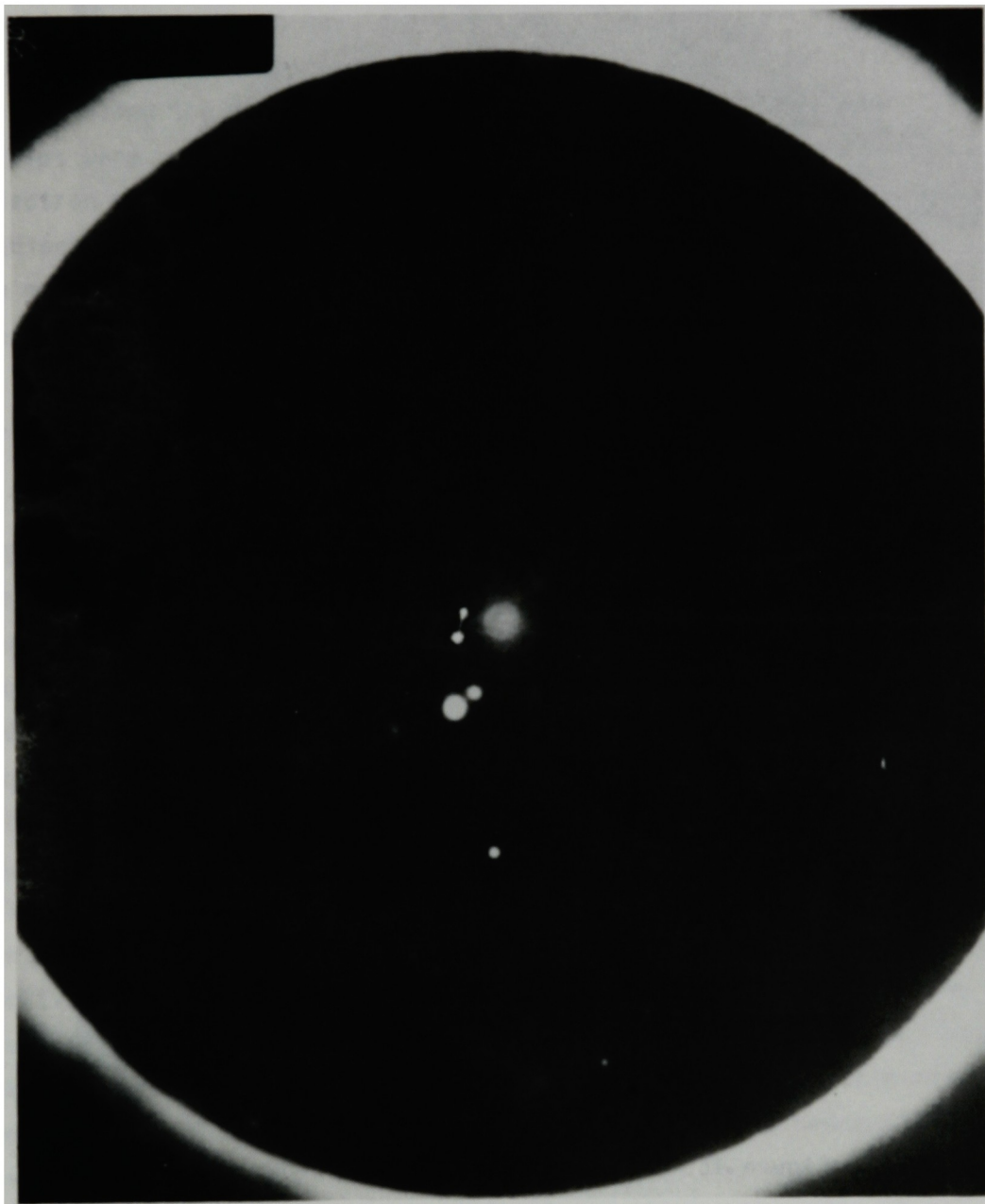
2.4.1 Sample Selection

The samples were obtained from the center of each quadrant of the plates, except for quadrant IV of Plate A. The surface deposit along one location in quadrant IV occurred at a tangent to the center of the



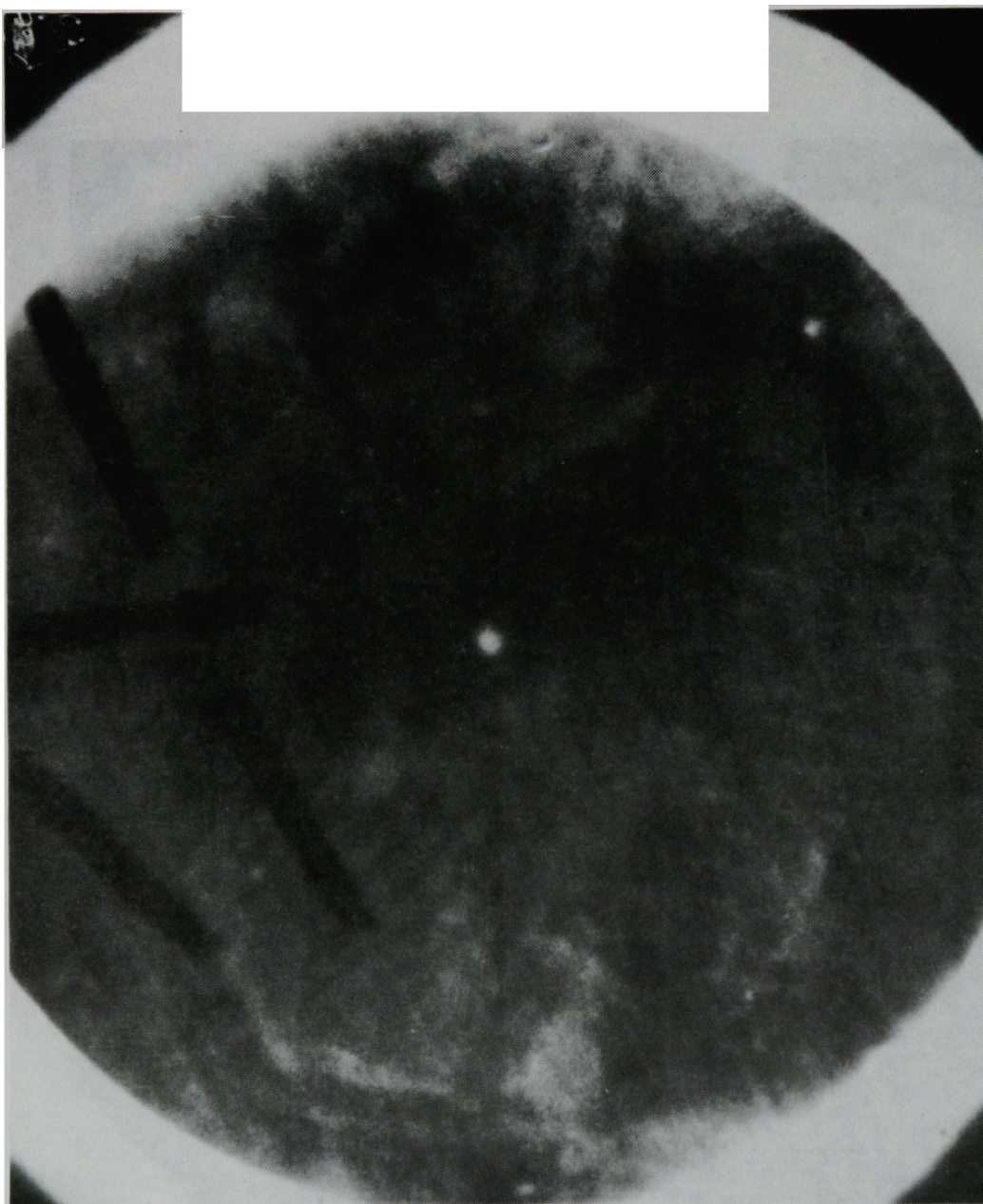
7-9660

Figure 14. Autoradiograph of plate A.



7-9861

Figure 15. Autoradiograph of plate B.



7-9662

Figure 16. Autoradiograph of plate P.

quadrant. Hence, the location of the samples from quadrant IV in Plate A was accordingly shifted from the center to include these surface deposits.

The first attempts to section the plates were made with a circular hole saw. Unfortunately, all these attempts were unsuccessful since the saw teeth frequently caught in the metal during cutting. Therefore, it was decided to use a band saw to cut through the plate from one edge to the other. As shown in Figure 17, a 1.59-cm-wide strip was cut through the plates along the center of the quadrants of each plate. After the two strips were cut from each plate, a 0.63-cm-wide section for optical and electron microscopy and a 1.27-cm-wide section for chemical and radiochemical analyses were obtained (Figure 18). The samples were stored in marked plastic vials. Table 2 lists the samples obtained and the surface areas measured for the analysis sample coupons.

2.4.2 Preparation of Samples for Analysis

After a review of potential dissolution methods, a destructive leach with radioactive tracers was chosen as the best method for the analysis of the surface deposits of the plate samples. In this method, the sample was supported with the surface to be leached in a solution (8 ml) containing both carrier and radioactive tracers. Stable strontium and iodine were added as carrier material and Sr-85 and I-131 as tracers. Following equilibration of the carrier and tracer with the surface-deposited species (this was determined to require 5-10 min), an unheated leach was begun. Multiple leaches were performed on samples A3 and P3 to determine the leach time required for the samples. It was determined that a cold leach period of approximately 4 h was required to place $\geq 97\%$ of the measurable activity in solution. The samples were then slowly heated and the I-129 volatilized and trapped in dilute NaOH (see Figure 19). Visual examination of the metal coupon after leaching indicated that all surface material had been removed from the leached surface. Although some redeposition was expected to occur, gross and isotopic radiation measurements indicated that the bulk of the activity had been removed. Upon completion of the leach process, the leach solution was diluted to 60 ml and stored in marked vials for subsequent chemical and radiochemical analyses.

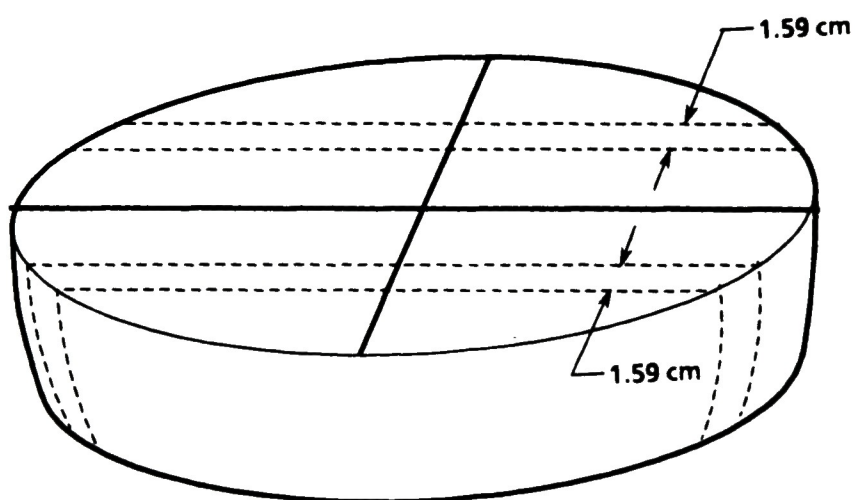


Figure 17. Sectioning plan for MCB plates.

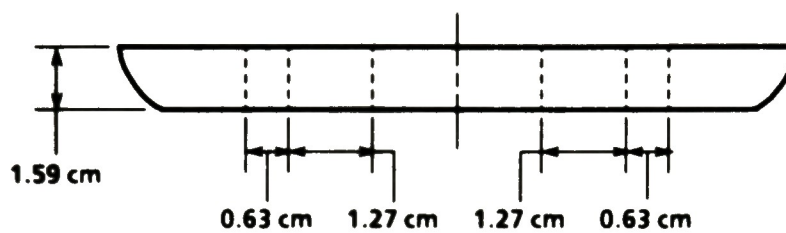


Figure 18. Sectioning plan for MCB plate samples for chemical analyses and metallography.

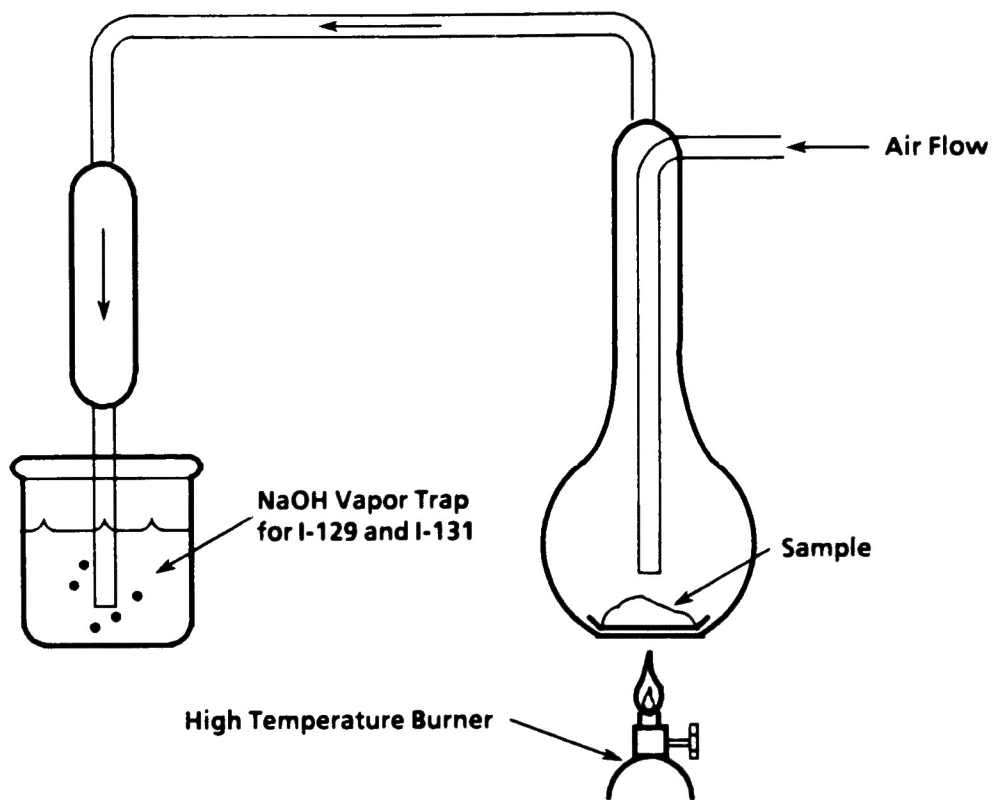


Figure 19. Schematic of I-129 volatilizing and trapping apparatus.

TABLE 2. LOCATION AND IDENTIFICATION OF SAMPLES OBTAINED AFTER SECTIONING OF THE MCB PLATES

| <u>Sample Number</u> | <u>Plate</u> | <u>Quadrant</u> | <u>Surface Dimensions</u> <u>(cm)</u> | <u>Surface Area</u> <u>(cm²)</u> |
|----------------------|--------------|-----------------|--|--|
| A1 | A | I | 1.31 x 1.50 | 1.97 |
| A2 | A | II | 1.45 x 1.37 | 1.99 |
| A3 | A | III | 1.40 x 1.34 | 1.88 |
| A4 | A | IV | 1.40 x 1.08 | 1.51 |
| B1 | B | I | 1.50 x 1.4 | 2.10 |
| B2 | B | II | 1.3 x 1.59 | 2.10 |
| B3 | B | III | 1.55 x 1.25 | 1.94 |
| B4 | B | IV | 1.3 x 1.51 | 2.00 |
| P1 | P | I | 1.3 x 1.46 | 1.90 |
| P2 | P | II | 1.22 x 1.3 | 1.59 |
| P3 | P | III | 1.5 x 1.25 | 1.88 |
| P4 | P | IV | 1.49 x 1.25 | 1.86 |

The bulk-diluted solutions were analyzed in a known geometry via gamma spectroscopy. All gamma spectroscopy analyses were performed using this system. Subsequently, aliquots were removed from the bulk solution for Sr-90 and I-129 analyses. A 5 ml sample was removed and subjected to a standard SrCO_3 precipitation separation⁵ followed by gamma spectroscopy for tracer measurements and liquid scintillation analysis (Packard TRICARB model). The radioiodine trapped in the NaOH was separated and was analyzed by gamma spectroscopy for a yield determination and subsequently activated using the Advanced Test Reactor (ATR) facility at the Idaho National Engineering Laboratory (INEL).

2.5 Fission Product Abundance and Distribution Analysis Results

Table 3 lists the total radionuclide content leached from the inner surface of each coupon. These data were decay-corrected to April 1, 1986. The A and B samples tend to have significantly higher concentrations (10-100 times) than the P samples, which appear to have come from an area of lower radionuclide surface deposition. Also, the Cs-137/Cs-134 ratio is less, which suggests that the deposited cesium comes from a different region of the core than that deposited in the A and B sample locations.

2.6 Core Material Abundance and Distribution

The abundance and distribution of core material in the surface deposits was determined: (a) by chemical analysis of the bulk diluted solutions of dissolved surface deposits for the presence of core materials and (b) by metallurgical analysis of polished cross sections of the surface deposits for the specific location of the core material in the surface deposit. The chemical analysis included inductively-coupled argon plasma spectroscopy (ICAP), atomic absorption spectroscopy (AAS), and spark source mass spectroscopy (SSMS) methods. The metallurgical analysis included optional metallography and scanning electron microscopy (SEM) methods.

Fold

out

ADONIS 1104 0 0 0

Sample Radionuclide Content
($\mu\text{Ci}/\text{cm}^2$)

| A2 | | A3--Leach 1 | | A3--Leach 2 | | A3--Leach 3 | | A4 | | B1 | | B2 | | B3 | | B4 | | P1 | | P2 | | P3 | | P3--Leach 2 | |
|-------|-----------------|-----------------|-----------------|-----------------|-----------------|------------------|------------------|------------------|-----------------|-----------------|-----------------|-----------------|-----------------|-----------------|-----------------|-----------------|-----------------|-----------------|-----------------|-----------------|-----------------|-----------------|-----------------|-----------------|-----------------|
| N | 3.5 hr Leach | 5.33 hr Leach | 4.0 hr Leach | 17 hr Leach | 4.5 hr Leach | 4 hr Leach | 7 hr Leach | 3 hr Leach | 5 hr Leach | 5 hr Leach | 5 hr Leach | 5 hr Leach | 5 hr Leach | 5 hr Leach | 5 hr Leach | 5 hr Leach | 5 hr Leach | 5 hr Leach | 5 hr Leach | 5 hr Leach | 5 hr Leach | 5 hr Leach | 5 hr Leach | 5 hr Leach | 5 hr Leach |
| E-2 | 5.92 ± 0.01 E-2 | 1.21 ± 0.44 E-2 | 3.12 ± 0.1 E-2 | b | 1.06 ± 0.02 E-1 | 4.44 ± 0.11 E-2 | 5.04 ± 0.05 E-2 | 3.67 ± 0.05 E-2 | 4.88 ± 0.05 E-2 | 2.30 ± 0.05 E-2 | 2.41 ± 0.05 E-2 | 1.63 | 2 | --b | 7.74 ± 1.18 E-4 | 3 | | | | | | | | | |
| E-2 | 1.04 ± 0.13 E-2 | 1.37 ± 0.22 E-1 | 0.14 ± 0.1 E-2 | 4.98 ± 0.77 E-3 | 3.02 ± 0.57 E-1 | 9.38 ± 1.43 E-2 | 1.76 ± 0.26 E-1 | 5.74 ± 0.87 E-2 | 6.30 ± 0.92 E-2 | 3.89 ± 0.57 E-1 | 3.91 ± 0.57 E-1 | 3.48 | 1 | --b | --b | --b | --b | --b | --b | --b | --b | --b | --b | --b | --b |
| 1 E-2 | 4.00 ± 0.35 E-2 | 2.52 ± 0.17 E-2 | --b | --b | 1.39 ± 0.01 E-0 | 2.59 ± 0.12 E-2 | 4.65 ± 0.17 E-2 | 1.76 ± 0.17 E-2 | 2.30 ± 0.23 E-2 | 4.12 ± 0.59 E-3 | --b | --b | --b | --b | --b | --b | --b | --b | --b | --b | --b | --b | --b | --b | --b |
| 1 E-6 | 1.28 ± 0.07 E-6 | 8.78 ± 1.01 E-7 | --b | --b | 1.87 ± 0.01 E-5 | 5.71 ± 0.06 E-2 | 5.83 ± 0.06 E-2 | 4.54 ± 0.06 E-2 | 6.75 ± 0.62 E-2 | 1.96 ± 0.12 E-3 | 1.84 ± 0.18 E-3 | 1.90 ± 0.12 E-3 | 2 | --b | --b | --b | --b | --b | --b | --b | --b | --b | --b | --b | --b |
| 2 E-1 | 1.61 ± 0.02 E-1 | 6.13 ± 0.12 E-2 | 6.93 ± 0.12 E-2 | 7.28 ± 0.25 E-3 | 1.39 ± 0.12 E-1 | 1.91 ± 0.005 E-0 | 2.03 ± 0.005 E-0 | 1.60 ± 0.005 E-0 | 2.35 ± 0.05 E-0 | 4.97 ± 0.05 E-2 | 4.92 ± 0.05 E-2 | 3.95 ± 0.05 E-2 | 3 | --b | --b | --b | --b | --b | --b | --b | --b | --b | --b | --b | --b |
| 5 E-0 | 5.72 ± 0.05 E-0 | 2.15 ± 0.01 E-0 | 2.46 ± 0.02 E-0 | 5.17 ± 0.05 E-0 | 5.17 ± 0.05 E-0 | 5.17 ± 0.05 E-0 | 5.17 ± 0.05 E-0 | 5.17 ± 0.05 E-0 | 5.17 ± 0.05 E-0 | 5.17 ± 0.05 E-0 | 5.17 ± 0.05 E-0 | 5.17 ± 0.05 E-0 | 5.17 ± 0.05 E-0 | 5.17 ± 0.05 E-0 | 5.17 ± 0.05 E-0 | 5.17 ± 0.05 E-0 | 5.17 ± 0.05 E-0 | 5.17 ± 0.05 E-0 | 5.17 ± 0.05 E-0 | 5.17 ± 0.05 E-0 | 5.17 ± 0.05 E-0 | 5.17 ± 0.05 E-0 | 5.17 ± 0.05 E-0 | 5.17 ± 0.05 E-0 | 5.17 ± 0.05 E-0 |

to April 1, 1986

y chemical separation and liquid scintillation analysis.

y neutron activation and subsequent gamma spectroscopy for the I-130 produced.

2.6.1 Inductively Coupled Argon Plasma Spectroscopy and Atomic Absorption Spectroscopy Analysis

Approximately 34 ml of the bulk-diluted solutions were analyzed by ICAP for the elements B, Na, Mg, Al, Si, Ca, Ti, V, Cr, Mn, Fe, Co, Ni, Cu, Zn, Zr, Mo, Ag, Cd, Sn, Sb, Te, and Pb using a computer-controlled Instrumentation Laboratories Model 200 Inductively Coupled Plasma Emission Spectrograph. Cs was determined by AAS, which is more sensitive for Cs than ICAP. The IL951 Atomic Absorption Spectrophotometer features double beam, dual wavelength measurement with selection of integration time plus peak area or height analysis.

The results are listed in Table 4. The high values for Fe, Cr, and Ni indicate that a significant amount of base metal was probably removed during the dissolution operation. On the other hand, there does appear to have been considerable transport of core materials and fission products, as indicated by the relatively high values for Ag, Cd, and Te, respectively.

2.6.2 Spark Source Mass Spectrometric Analysis

Five milliliter aliquots from the original diluted solutions were analyzed with an AEI Model MS702R SSMS instrument. Typical results from each of the three plates are given in Table 5.

2.6.3 Metallography

The samples for metallography were mounted, ground, and polished using SiC and Al₂O₃ abrasives. The surface deposit cross sections were examined with an Olympus microscope. Black and white photographs were obtained from each sample.

Figures 20-22 show the optical micrographs for each specimen. A thin surface layer (4-12 μ m) is visible on the specimens from plates B and P, but this layer is less than 2 μ m thick on the specimens from quadrants I-III of Plate A (samples A1, A2, and A3). The surface layer on sample A4 is clearly thicker (3-4 μ m) than on samples A1, A2, and A3,

TABLE 4. MCB PLATE SAMPLES ELEMENTAL SURFACE CONCENTRATIONS

| Element | Concentration in Sample (mg/cm ²) | | | | | | | | | | | | | | |
|---------|--|---------|---------|---------|---------|--------|---------|---------|---------|---------|---------|--------|---------|---------|---------|
| | A1 | A2 | A3-1 | A3-2 | A3-3 | A4 | B1 | B2 | B3 | B4 | P1 | P2 | P3-1 | P3-2 | P4 |
| Li | <0.012 | <0.012 | <0.013 | <0.013 | <0.013 | <0.016 | <0.011 | <0.011 | <0.012 | <0.012 | <0.013 | <0.015 | <0.013 | <0.013 | <0.013 |
| B | 0.017 | 0.003 | 0.018 | <0.002 | 0.002 | <0.002 | <0.001 | <0.001 | 0.004 | <0.002 | 0.009 | <0.002 | <0.002 | <0.002 | <0.002 |
| Na | 1.1 | 1.2 | 1.020 | 0.77 | 0.73 | 2.0 | 1.4 | 0.54 | 1.1 | 0.90 | 0.51 | 0.60 | 1.2 | 1.2 | 1.3 |
| Mg | <0.045 | <0.045 | <0.048 | <0.048 | <0.048 | <0.060 | <0.043 | <0.043 | <0.046 | <0.045 | <0.047 | <0.056 | <0.048 | 0.086 | <0.048 |
| Al | 0.093 | <0.045 | <0.048 | <0.048 | 0.067 | 0.083 | <0.043 | <0.043 | <0.046 | <0.045 | <0.047 | <0.056 | <0.048 | <0.048 | 0.052 |
| Si | <0.3 | <0.3 | <0.3 | 0.77 | <0.3 | <0.4 | 0.83 | 0.97 | <0.31 | <0.30 | <0.32 | <0.38 | <0.32 | <0.32 | <0.32 |
| P | 8.67 | 1.9 | 0.54 | 1.8 | 1.2 | 4.05 | 2.1 | 3.09 | 1.4 | 12.2 | 4.04 | 2.5 | 4.05 | 5.74 | 2.48 |
| K | 9.3 | 4.1 | 4.4 | 4.3 | 4.4 | 6.0 | 2.7 | 2.1 | 3.0 | 7.29 | 3.95 | 4.24 | 3.54 | 4.56 | 4.03 |
| Ca | 0.021 | 0.10 | 0.19 | 0.064 | 0.086 | 0.064 | 0.019 | 0.034 | 0.036 | 0.023 | 0.057 | 0.045 | 0.080 | 1.4 | 0.031 |
| Ti | <0.030 | <0.030 | <0.032 | <0.032 | <0.032 | <0.040 | <0.029 | <0.029 | <0.031 | <0.030 | <0.032 | <0.038 | <0.032 | <0.032 | <0.032 |
| V | 0.28 | 0.18 | 0.11 | 0.070 | 0.18 | 0.22 | 0.9 | 1.0 | 0.18 | 0.14 | 0.23 | 0.33 | 0.17 | 0.073 | 0.21 |
| Cr | 12.0 | 8.1 | 5.1 | 7.21 | 10.4 | 10.7 | 8.94 | 49.1 | 8.38 | 9.42 | 13.8 | 15.8 | 8.87 | 8.43 | 9.84 |
| Mn | 0.69 | 0.51 | 0.29 | 0.38 | 0.61 | 0.60 | 0.40 | 2.6 | 0.40 | 0.48 | 0.76 | 0.94 | 0.48 | 0.45 | 0.52 |
| Fe | 53.0 | 32.1 | 25.3 | 32.1 | 44.1 | 44.9 | 36.5 | 188.0 | 35.4 | 40.4 | 47.7 | 65.6 | 36.9 | 34.7 | 43.8 |
| Co | 0.051 | 0.033 | 0.022 | 0.032 | 0.038 | 0.004 | 0.021 | 0.19 | 0.028 | 0.003 | 0.005 | 0.068 | 0.035 | 0.045 | 0.048 |
| Ni | 6.39 | 4.31 | 2.7 | 3.80 | 5.33 | 5.44 | 4.66 | 25.8 | 4.58 | 5.16 | 7.26 | 8.21 | 4.72 | 4.56 | 5.26 |
| Cu | 0.23 | 0.15 | 0.080 | 0.096 | 0.18 | 0.18 | 0.17 | 0.971 | 0.12 | 0.14 | 0.095 | 0.13 | <0.016 | 0.064 | 0.016 |
| Zn | <0.015 | <0.015 | 0.032 | <0.016 | <0.016 | <0.020 | <0.014 | <0.014 | <0.015 | <0.015 | <0.016 | <0.019 | <0.016 | 0.032 | <0.016 |
| Sr | | | | | | | | | | | | | | | |
| Zr | <0.15 | <0.15 | <0.16 | <0.16 | <0.16 | <0.20 | 0.15 | <0.14 | <0.15 | <0.15 | <0.16 | <0.19 | <0.16 | <0.16 | <0.16 |
| Mo | 0.12 | 0.069 | 0.045 | 0.073 | 0.096 | 0.12 | 0.074 | 0.40 | 0.077 | 0.078 | 0.088 | 0.083 | 0.038 | 0.064 | 0.042 |
| Ag | 1.38 | <0.3 | 0.48 | 0.57 | 0.41 | 0.72 | 0.63 | 4.40 | <0.31 | 0.51 | 1.4 | 1.1 | 0.86 | <0.31 | 0.39 |
| Cd | 0.0006 | 0.00075 | 0.00048 | <0.0002 | <0.0002 | 0.026 | 0.00029 | <0.0001 | <0.0002 | <0.0002 | <0.0002 | 0.0004 | <0.0002 | <0.0002 | 0.00048 |
| Sn | 0.015 | 0.006 | 0.0013 | 0.006 | 0.006 | 0.044 | 0.011 | 0.054 | 0.03 | 0.006 | 0.02 | 0.008 | 0.006 | 0.019 | 0.006 |
| Sb | <0.006 | <0.006 | <0.006 | <0.006 | <0.006 | <0.008 | <0.006 | <0.006 | <0.006 | <0.006 | <0.006 | <0.008 | <0.006 | <0.006 | <0.006 |
| Te | <0.015 | 0.033 | <0.016 | <0.016 | <0.016 | 0.028 | <0.014 | 0.13 | <0.015 | 0.045 | 0.035 | 0.045 | <0.016 | <0.016 | 0.045 |
| Cs | <0.075 | <0.075 | <0.080 | <0.080 | <0.080 | <0.099 | <0.071 | <0.071 | <0.077 | <0.075 | <0.079 | <0.094 | <0.080 | <0.080 | <0.080 |
| Pb | <0.6 | <0.6 | 1.5 | <0.6 | 1.3 | 3.0 | <0.6 | <0.6 | <0.6 | 2.8 | <0.6 | 1.4 | <0.6 | 1.1 | <0.6 |

TABLE 5. MASS SPECTROMETRIC ANALYSIS OF MCB PLATE SAMPLES

| Element | Elemental Concentration in Sample ($\mu\text{g}/\text{cm}^2$) | | | | | | |
|---------|--|-----------|-----------|-----------|-----------|-----------|-----------|
| | A1 | A2 | A3-1 | B1 | B2 | P1 | P3-2 |
| Li | 1.52 E-4 | 3.02 E-4 | 6.38 E-5 | 8.57 E-4 | 8.57 E-4 | 3.16 E-4 | 3.19 E-4 |
| Be | <1.83 E-4 | <1.81 E-5 | <1.28 E-5 | <2.86 E-5 | <1.71 E-5 | <1.89 E-5 | <1.91 E-5 |
| B | 1.52 E-2 | 1.81 E-2 | 3.19 E-3 | 2.86 E-2 | 4.29 E-2 | 6.32 E-2 | 9.57 E-3 |
| F | 1.83 E-2 | 1.81 E-2 | 3.19 E-2 | 5.71 E-3 | 1.71 E-2 | 9.47 E-3 | 1.91 E-2 |
| Na | 1.22 E+1 | 6.03 E+0 | 1.60 E+3 | 2.86 E+0 | 8.57 E+0 | 3.16 E+0 | 9.57 E+0 |
| Mg | 1.22 E-2 | 3.02 E-2 | 2.23 E-2 | 4.29 E-2 | 1.14 E-2 | 3.16 E-2 | 3.19 E-1 |
| Al | 4.57 E-2 | 4.52 E-2 | 4.79 E-2 | 8.57 E-2 | 4.29 E-2 | 3.16 E-1 | 4.79 E-2 |
| Si | 6.09 E-1 | 9.05 E-1 | 3.19 E-1 | 4.29 E+0 | 8.57 E-1 | 1.58 E+0 | 4.79 E-1 |
| P | 6.09 E-3 | 6.03 E-3 | 9.57 E-3 | 1.43 E-1 | 5.71 E-3 | 2.21 E-2 | 2.23 E-2 |
| S | 3.05 E-1 | 3.02 E+0 | 6.38 E-2 | 4.29 E-1 | 2.86 E+0 | 3.16 E-1 | 3.19 E+0 |
| Cl | 6.09 E+1 | 4.52 E+1 | 1.28 E+3 | 2.86 E+2 | 8.57 E+1 | 2.21 E-2 | 2.23 E+2 |
| K | 9.14 E-0 | 4.52 E+0 | 3.19 E+0 | 1.14 E+1 | 8.57 E+0 | 9.47 E+0 | 9.57 E+0 |
| Ca | 3.05 E-1 | 9.05 E-1 | 3.19 E-2 | 8.57 E-1 | 2.86 E-1 | 6.32 E-1 | 3.19 E+1 |
| Sc | <1.52 E-3 | 1.21 E-3 | 6.38 E-4 | 2.86 E-3 | 1.71 E-3 | 2.21 E-3 | 1.91 E-3 |
| Ti | <1.83 E-3 | 1.81 E-3 | 3.19 E-4 | 1.14 E-2 | 2.86 E-3 | 3.16 E-3 | 3.19 E-3 |
| V | 6.09 E-2 | 4.52 E-3 | 4.79 E-3 | 4.29 E-1 | 4.29 E-2 | 6.32 E-2 | 3.19 E-2 |
| Cr | 3.05 E+1 | 1.21 E+1 | 9.57 E-1 | 5.71 E+1 | 2.86 E+1 | 3.16 E+1 | 3.19 E+1 |
| Mn | 6.09 E-0 | 4.52 E+0 | 1.28 E-1 | 1.43 E+1 | 2.86 E+0 | 6.32 E+0 | 4.79 E+0 |
| Fe | 6.09 E+1 | 3.02 E+1 | 2.23 E+0 | 2.86 E+2 | 1.14 E+2 | 1.26 E+2 | 1.28 E+2 |
| Co | 2.13 E-1 | 1.21 E-1 | 4.79 E-3 | 1.14 E+0 | 1.14 E-1 | 2.21 E-1 | 1.28 E-1 |
| Ni | 1.83 E+1 | 1.21 E+1 | 4.79 E-1 | 1.14 E+2 | 1.14 E+1 | 1.89 E+1 | 1.28 E+1 |
| Cu | 4.57 E-1 | 3.02 E-1 | 2.23 E-2 | 1.71 E+0 | 5.71 E-1 | 4.74 E-1 | 3.19 E-1 |
| Zn | 3.05 E-2 | 3.02 E-2 | 4.79 E-3 | 4.29 E-1 | 1.14 E-1 | 1.26 E-1 | 1.91 E-1 |
| Ga | <3.05 E-4 | <3.02 E-4 | <1.91 E-4 | <4.29 E-4 | <2.86 E-4 | <3.16 E-4 | <3.19 E-4 |
| Ge | <4.57 E-3 | <4.52 E-3 | <3.19 E-3 | <5.71 E-3 | <4.29 E-3 | <4.74 E-3 | <4.79 E-3 |

TABLE 5. (continued)

| Element | Elemental Concentration in Sample ($\mu\text{g}/\text{cm}^2$) | | | | | | |
|---------|--|-----------|-----------|-----------|-----------|-----------|-----------|
| | A1 | A2 | A3-1 | B1 | B2 | P1 | P3-2 |
| As | <1.83 E-4 | <1.81 E-4 | <1.60 E-4 | <2.86 E-4 | <1.71 E-4 | <1.89 E-4 | <1.91 E-4 |
| Se | <6.09 E-4 | <6.03 E-4 | <9.57 E-4 | <8.57 E-4 | <5.71 E-4 | <6.32 E-4 | <6.38 E-4 |
| Br | <1.52 E-3 | <1.51 E-3 | <1.60 E-3 | <2.00 E-3 | <1.43 E-3 | <1.58 E-3 | <1.60 E-3 |
| Rb | <1.83 E-4 | <1.81 E-4 | <1.09 E-3 | <1.43 E-3 | <1.71 E-4 | <1.89 E-4 | <1.91 E-4 |
| Sr | 1.22 E+1 | 6.03 E-0 | 6.38 E-1 | 2.86 E+1 | 1.14 E+1 | 2.21 E+1 | 1.28 E+1 |
| Y | <4.57 E-4 | <4.52 E-4 | <3.19 E-4 | <5.71 E-4 | <4.29 E-4 | <4.74 E-4 | <4.79 E-4 |
| Zr | <9.14 E-4 | <9.05 E-4 | <1.60 E-3 | <1.43 E-3 | <8.57 E-4 | <9.47 E-4 | <9.47 E-4 |
| Nb | 3.05 E-2 | 1.21 E-2 | 1.28 E-3 | 8.57 E-2 | 1.14 E-2 | 1.26 E-2 | 3.19 E-3 |
| Mo | 1.52 E-1 | 9.05 E-2 | 3.19 E-3 | 1.14 E+0 | 8.57 E-2 | 9.47 E-2 | 6.38 E-2 |
| Ru | <1.52 E-3 | <1.51 E-3 | <9.57 E-4 | <1.71 E-3 | <1.43 E-3 | <1.58 E-3 | <1.60 E-3 |
| Rh | <6.09 E-4 | <6.03 E-4 | <3.19 E-4 | <8.57 E-4 | <5.71 E-4 | <6.32 E-4 | <6.38 E-4 |
| Pd | <1.83 E-3 | <1.81 E-3 | <9.57 E-4 | <2.86 E-3 | <1.71 E-3 | <1.89 E-3 | <1.91 E-3 |
| Ag | <3.05 E-4 | <3.02 E-4 | <4.79 E-4 | <4.29 E-4 | <2.86 E-4 | <3.16 E-4 | <3.19 E-4 |
| Cd | <1.22 E-2 | <1.21 E-2 | <9.57 E-3 | <1.43 E-2 | <1.14 E-2 | <1.26 E-2 | <1.28 E-2 |
| In | <3.05 E-4 | <3.02 E-4 | <3.19 E-4 | <4.29 E-3 | <2.86 E-3 | <3.16 E-4 | <4.79 E-4 |
| Sn | <1.83 E-3 | <1.81 E-3 | <9.57 E-4 | <8.57 E-3 | <4.29 E-3 | <1.89 E-3 | <1.91 E-3 |
| Sb | <9.14 E-3 | <9.05 E-3 | <3.19 E-4 | <1.14 E-2 | <8.57 E-3 | <1.26 E-2 | <9.57 E-3 |
| Te | <1.83 E-3 | <1.81 E-3 | <4.79 E-3 | <2.86 E-3 | <1.71 E-3 | <1.89 E-3 | <1.91 E-3 |
| I | <9.14 E-3 | <9.05 E-3 | <1.60 E-3 | <1.14 E-2 | <8.57 E-3 | <9.47 E-3 | <9.57 E-3 |
| Cs | <6.09 E-5 | <6.03 E-5 | <9.57 E-4 | <1.43 E-4 | <8.57 E-5 | <6.32 E-5 | <9.57 E-5 |
| Ba | <9.14 E-4 | <9.05 E-4 | <3.19 E-3 | <1.43 E-3 | <8.57 E-4 | <9.47 E-4 | <9.57 E-4 |
| La | <6.09 E-4 | <6.03 E-4 | <3.19 E-3 | <1.43 E-3 | <5.71 E-4 | <6.32 E-4 | <6.38 E-4 |
| Ce | <3.05 E-4 | <3.02 E-4 | <3.19 E-4 | <4.29 E-4 | <2.86 E-4 | <3.16 E-4 | <3.19 E-4 |
| Pr | <6.09 E-4 | <6.03 E-4 | <3.19 E-3 | <1.43 E-3 | <8.57 E-4 | <9.47 E-4 | <9.57 E-4 |
| Nd | <6.09 E-3 | <6.03 E-3 | <3.19 E-3 | <5.71 E-3 | <4.29 E-3 | <4.74 E-4 | <4.79 E-3 |

TABLE 5. (continued)

| Element | Elemental Concentration in Sample ($\mu\text{g}/\text{cm}^2$) | | | | | | |
|---------|--|-----------|-----------|-----------|-----------|-----------|-----------|
| | A1 | A2 | A3-1 | B1 | B2 | P1 | P3-2 |
| Sm | <1.83 E-3 | <1.81 E-3 | <1.60 E-3 | <2.86 E-3 | <1.71 E-3 | <1.89 E-3 | <1.91 E-3 |
| Eu | <1.52 E-3 | <1.51 E-3 | <9.57 E-4 | <1.71 E-3 | <1.43 E-3 | <1.58 E-3 | <1.60 E-3 |
| Gd | <1.83 E-3 | <1.81 E-3 | <1.60 E-3 | <2.86 E-3 | <1.71 E-3 | <1.89 E-3 | <1.91 E-3 |
| Tb | <6.09 E-4 | <6.03 E-4 | <3.19 E-4 | <8.57 E-4 | <5.71 E-4 | <6.32 E-4 | <6.38 E-4 |
| Dy | <1.83 E-3 | <1.81 E-3 | <1.60 E-3 | <2.86 E-3 | <1.71 E-3 | <1.89 E-3 | <1.91 E-3 |
| Ho | <9.14 E-4 | <9.05 E-4 | <4.79 E-4 | <1.43 E-3 | <8.57 E-4 | <9.47 E-4 | <9.57 E-4 |
| Er | <1.83 E-3 | <1.81 E-3 | <9.57 E-4 | <2.86 E-3 | <1.71 E-3 | <1.89 E-3 | <1.91 E-3 |
| Tm | <9.14 E-4 | <9.05 E-4 | <4.79 E-4 | <1.43 E-3 | <8.57 E-4 | <9.47 E-4 | <9.57 E-4 |
| Yb | <1.83 E-3 | <1.81 E-3 | <1.60 E-3 | <2.86 E-3 | <1.71 E-3 | <1.89 E-3 | <1.91 E-3 |
| Lu | <9.14 E-4 | <9.05 E-4 | <4.79 E-4 | <1.43 E-3 | <8.57 E-4 | <9.47 E-4 | <9.57 E-4 |
| Hf | <1.83 E-3 | <1.81 E-3 | <9.57 E-3 | <2.86 E-3 | <1.71 E-3 | <1.89 E-3 | <1.91 E-3 |
| Ta | <1.52 E-3 | <1.51 E-3 | <9.57 E-4 | <1.43 E-2 | <5.71 E-3 | <1.58 E-3 | <1.60 E-3 |
| W | <1.83 E-3 | <1.81 E-3 | <1.60 E-3 | <4.29 E-2 | <1.71 E-3 | <3.16 E-3 | <1.91 E-3 |
| Re | <1.83 E-3 | <1.81 E-3 | <9.57 E-4 | <2.86 E-3 | <1.71 E-3 | <1.89 E-3 | <1.91 E-3 |
| Os | <1.83 E-3 | <1.81 E-3 | <9.57 E-4 | <2.86 E-3 | <1.71 E-3 | <1.89 E-3 | <1.91 E-3 |
| Ir | <1.83 E-3 | <1.81 E-3 | <9.57 E-4 | <2.86 E-3 | <1.71 E-3 | <1.89 E-3 | <1.91 E-3 |
| Pt | <1.83 E-3 | <1.81 E-3 | <1.60 E-3 | <2.86 E-3 | <1.71 E-3 | <1.89 E-3 | <1.91 E-3 |
| Au | <9.14 E-4 | <9.05 E-4 | <4.79 E-3 | <1.43 E-3 | <8.57 E-4 | <9.47 E-4 | <9.57 E-4 |
| Hg | <4.57 E-2 | <4.52 E-2 | <1.60 E-2 | <5.71 E-2 | <4.29 E-2 | <4.74 E-3 | <4.79 E-2 |
| Tl | <3.05 E-3 | <3.02 E-3 | <9.57 E-4 | <4.29 E-3 | <2.86 E-3 | <3.16 E-3 | <3.19 E-3 |
| Pb | <1.83 E-3 | <1.81 E-3 | <1.91 E-3 | <8.57 E-2 | <1.71 E-3 | <1.89 E-3 | <1.91 E-3 |
| Bi | <9.14 E-4 | <9.05 E-4 | <4.79 E-4 | <1.43 E-3 | <8.57 E-4 | <9.47 E-4 | <9.57 E-4 |
| Th | <1.83 E-3 | <1.81 E-3 | <1.60 E-3 | <2.86 E-3 | <1.71 E-3 | <1.89 E-3 | <1.91 E-3 |
| U | <9.14 E-4 | <9.05 E-4 | <1.60 E-3 | <1.43 E-3 | <8.57 E-4 | <9.47 E-4 | <9.57 E-4 |

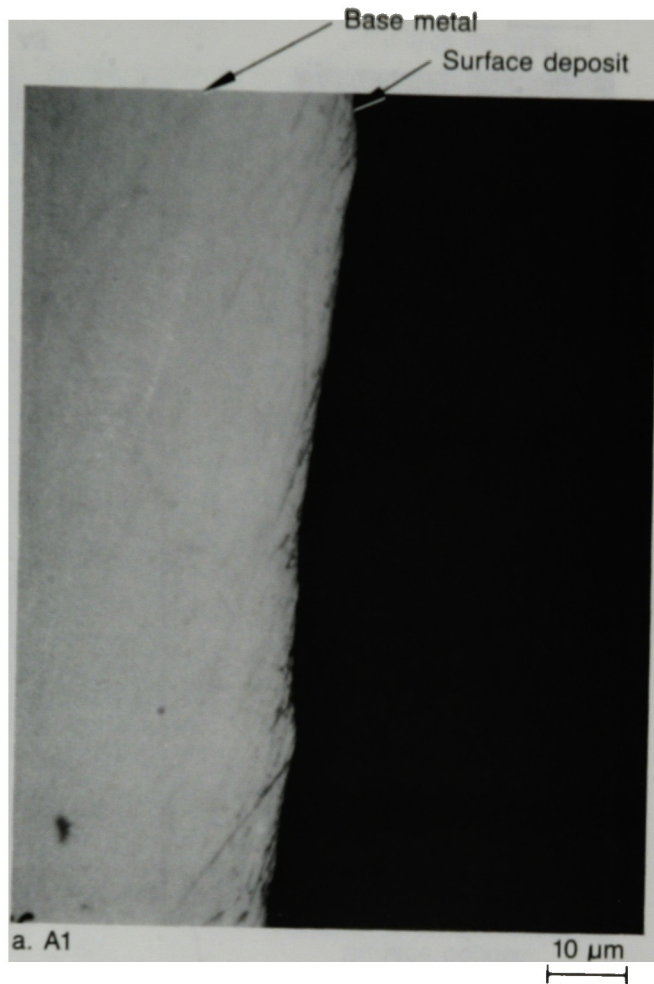


Figure 20a and b. Optical micrographs of specimens from plate A.

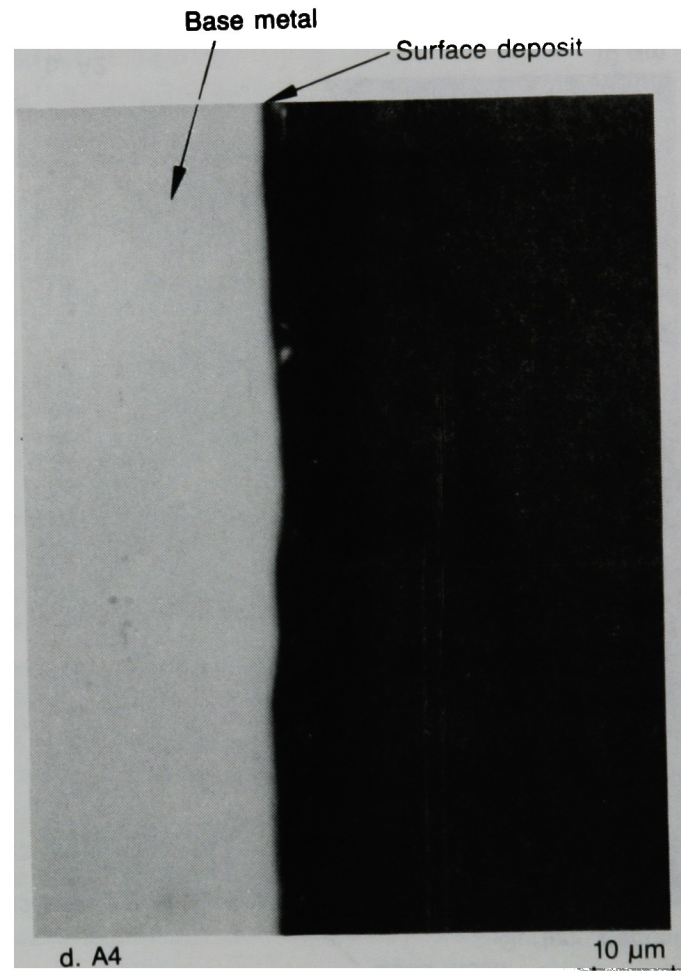
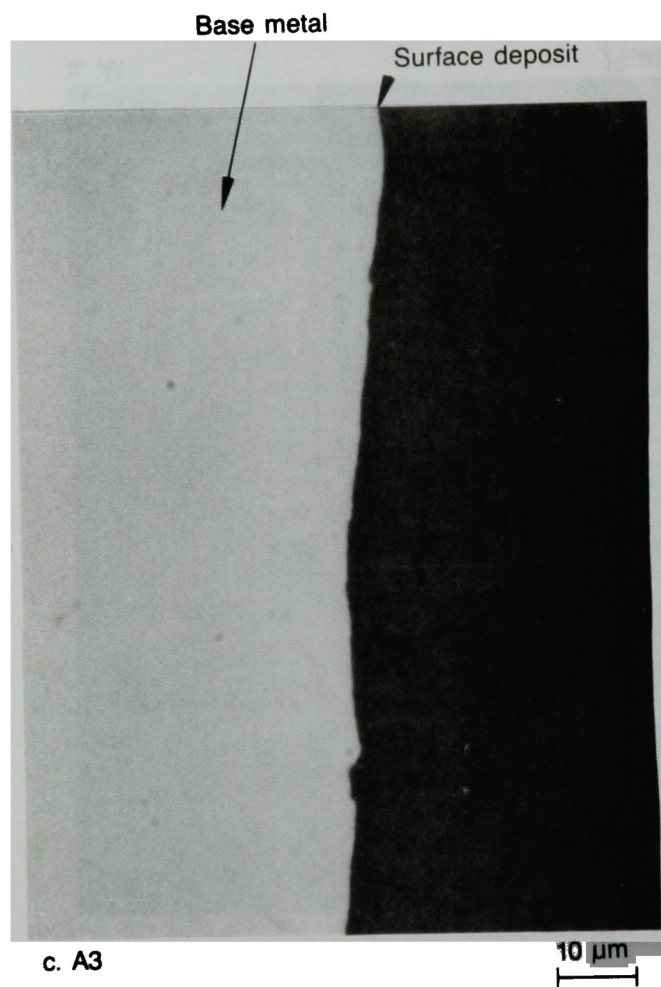


Figure 20c and d. Optical micrographs of specimens from plate A.

Base metal

Surface deposit



10 μ m

a. B1

Base metal

Surface deposit



10 μ m

b. B2

Figure 21a and b. Optical micrographs of specimens from plate B.

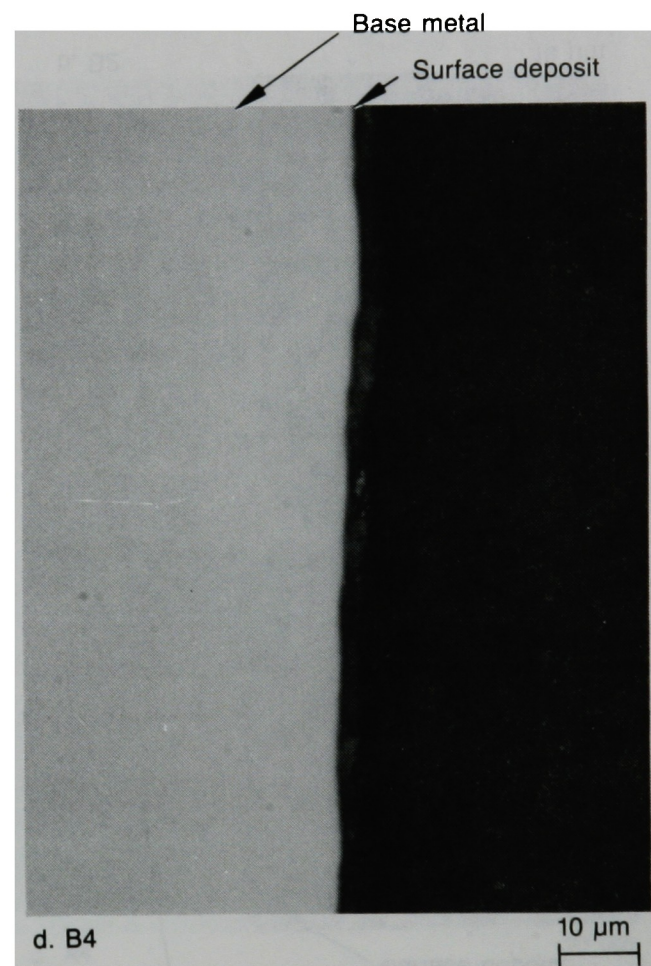
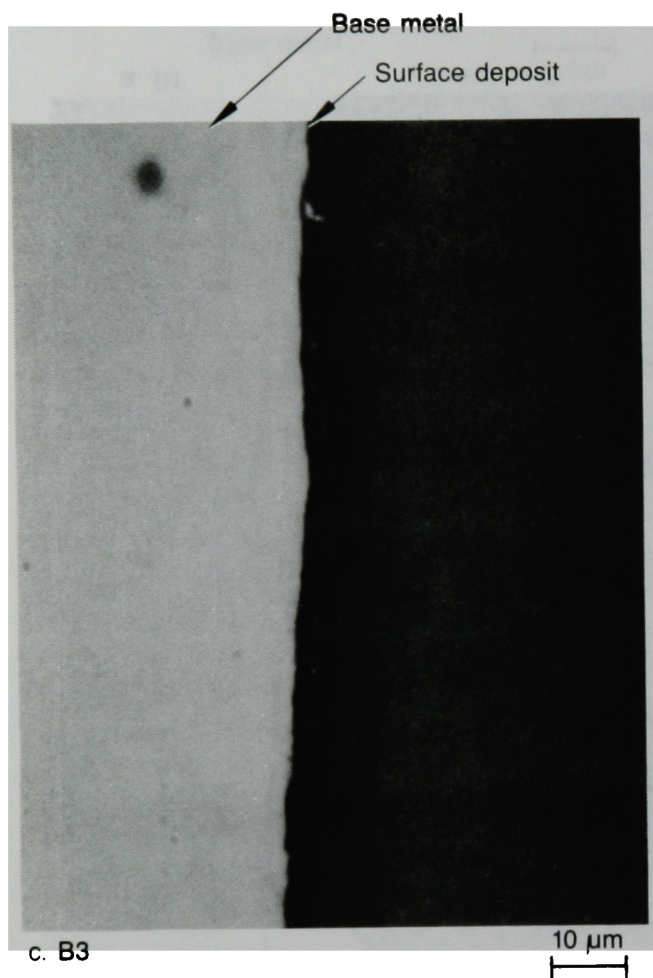


Figure 21c and d. Optical micrographs of specimens from plate B.

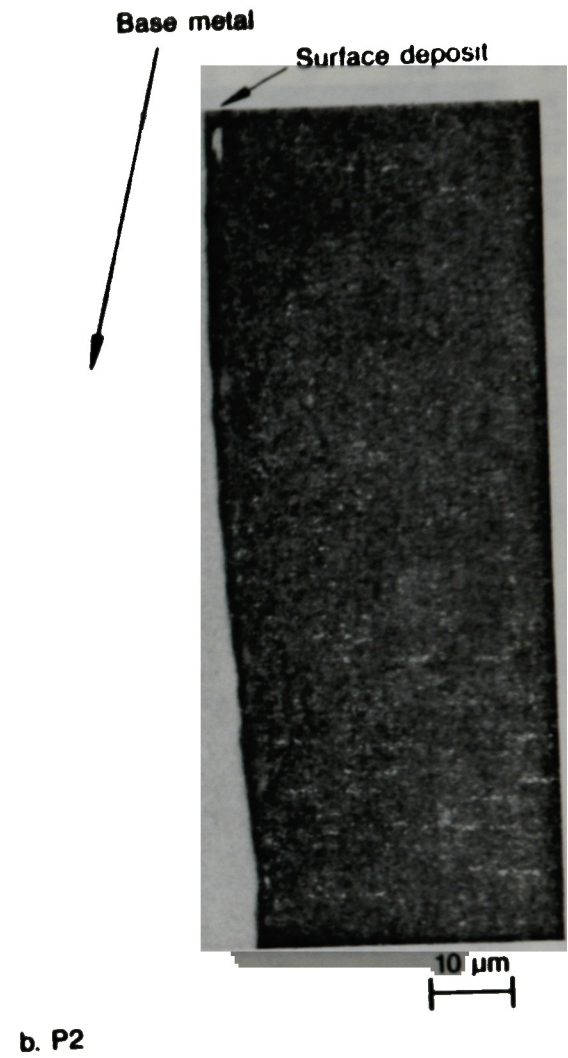
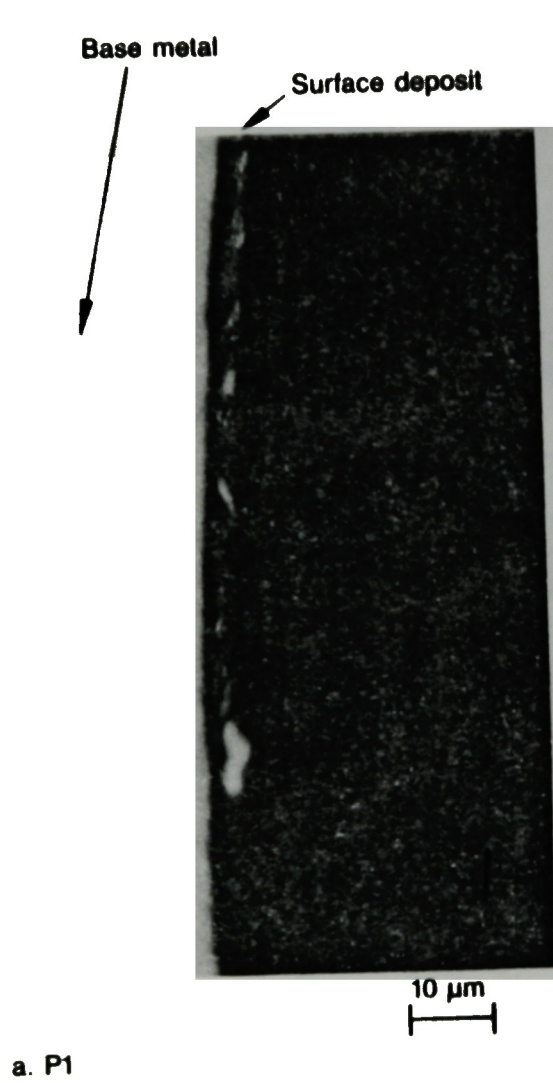
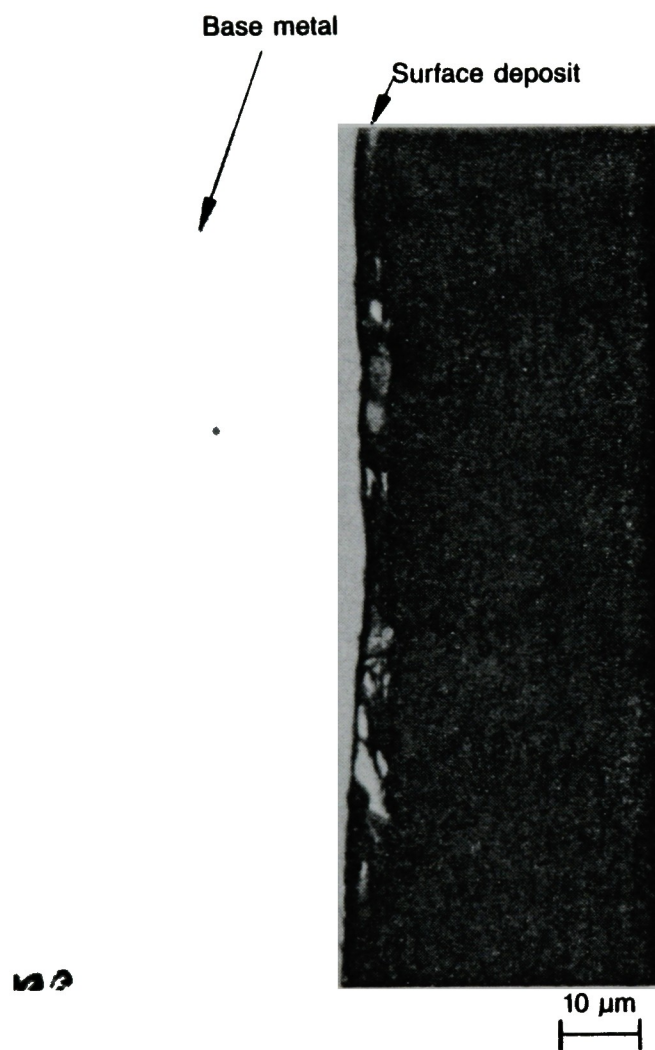
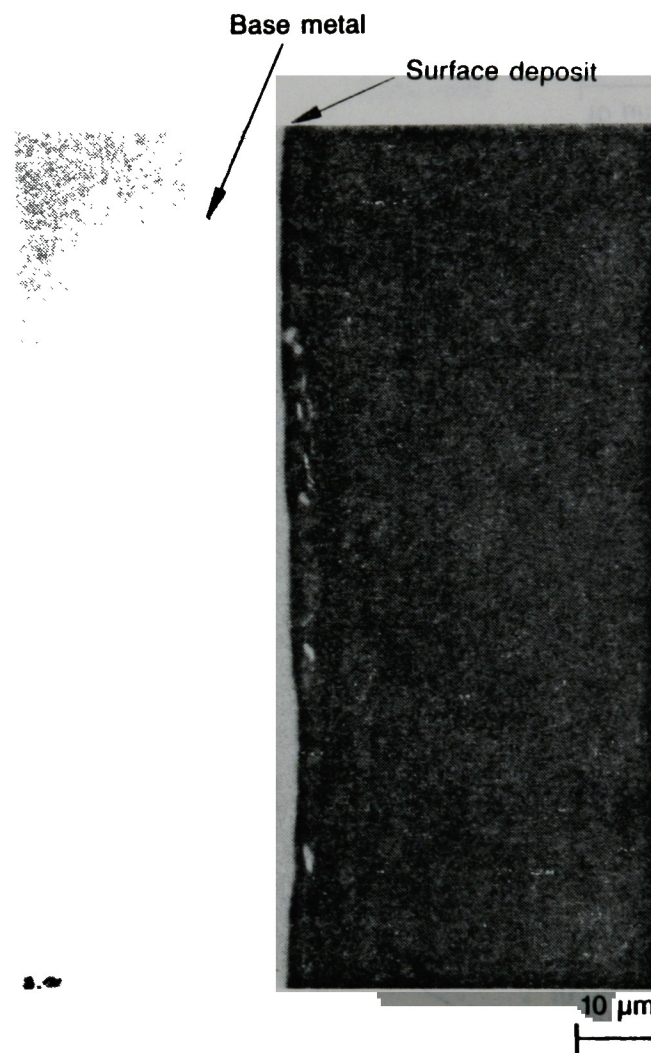


Figure 22a and b. Optical micrographs of specimens from plate P.



c. P3



d. P4

Figure 22c and d. Optical micrographs of specimens from plate P.

which agrees with the visual examinations. On each sample, however, there were no measurable differences in the thickness within the surface layers.

2.6.4 Scanning Electron Microscopy

To identify the surface layers on the metallographic samples, the samples were examined with an ISI Model 100 SEM equipped with a Tracor Northern energy dispersive system (EDS) analyzer.

Detailed examination of the samples showed no major differences in the structure and morphology of the surface layer within each sample. Typical SEM micrographs of the samples are shown in Figures 23-25. As can be seen, the surface layers are relatively thin. Not surprisingly, EDS analysis of the surface layer showed it to consist mainly of Fe, Cr, and Ni (Figures 23c, 24b, and 25b). The proximity of the matrix elements Fe, Cr, and Ni will tend to overwhelm the electron energy peaks from any other element. However, the presence of In and/or Sn was also revealed in Specimens A1 and A4 (Figures 23b and 26a, b, and c). Since EDS cannot resolve the electron energy peaks of In and Sn, electron microprobe (wavelength dispersive) analysis was also performed on specimen A4 to resolve any uncertainties. As Figure 26d shows, both Sn and In are unambiguously present in the surface layer of the specimen.

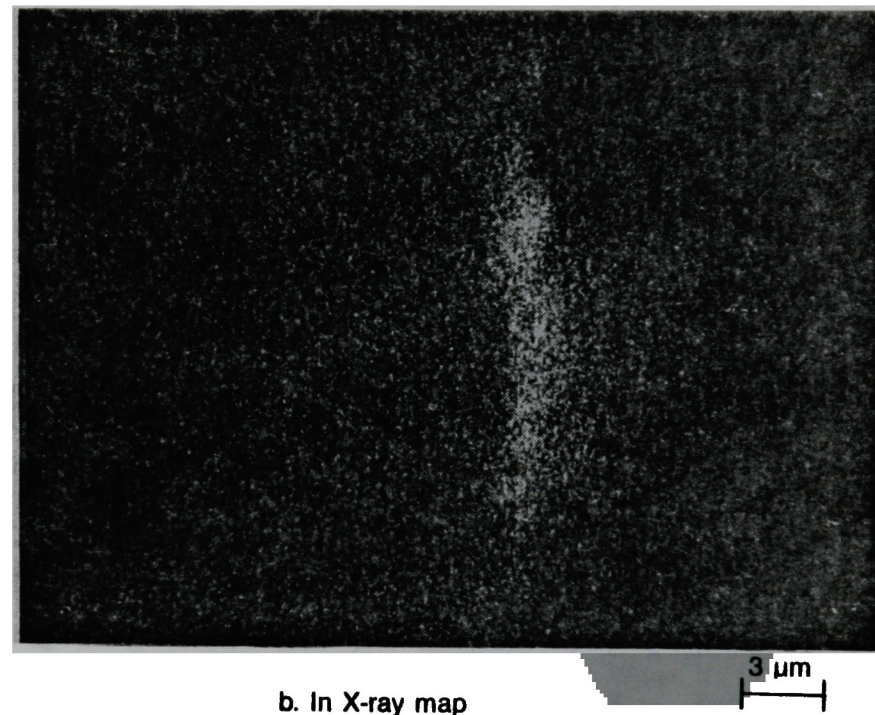
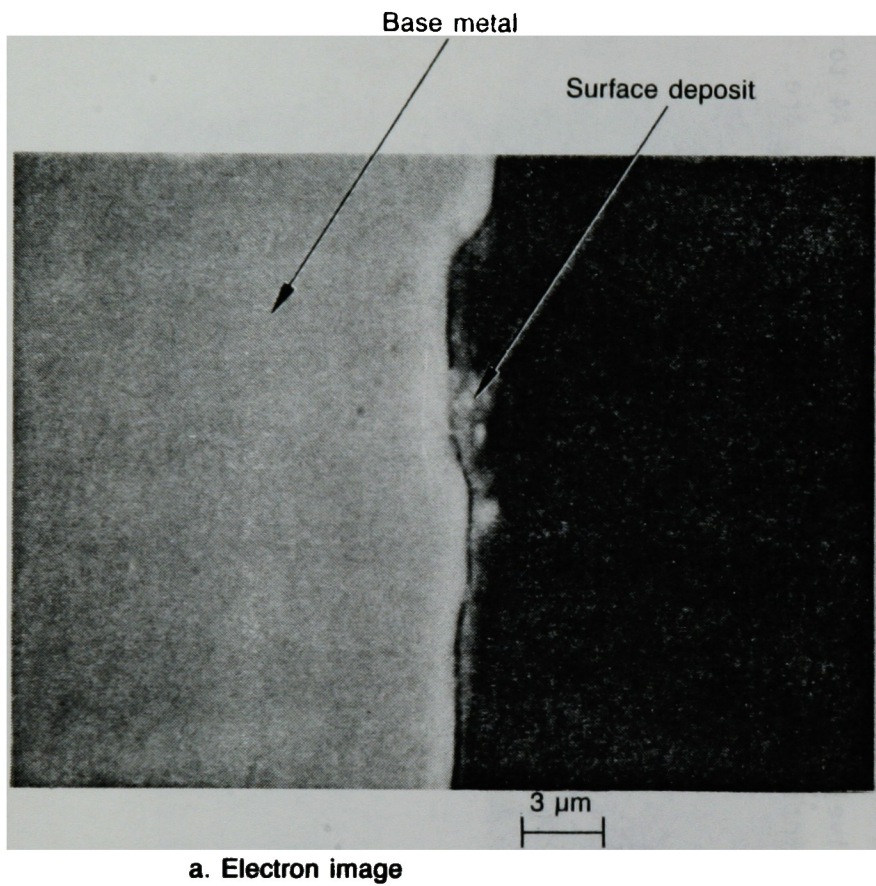


Figure 23a and b. SEM photographs of specimen A1.

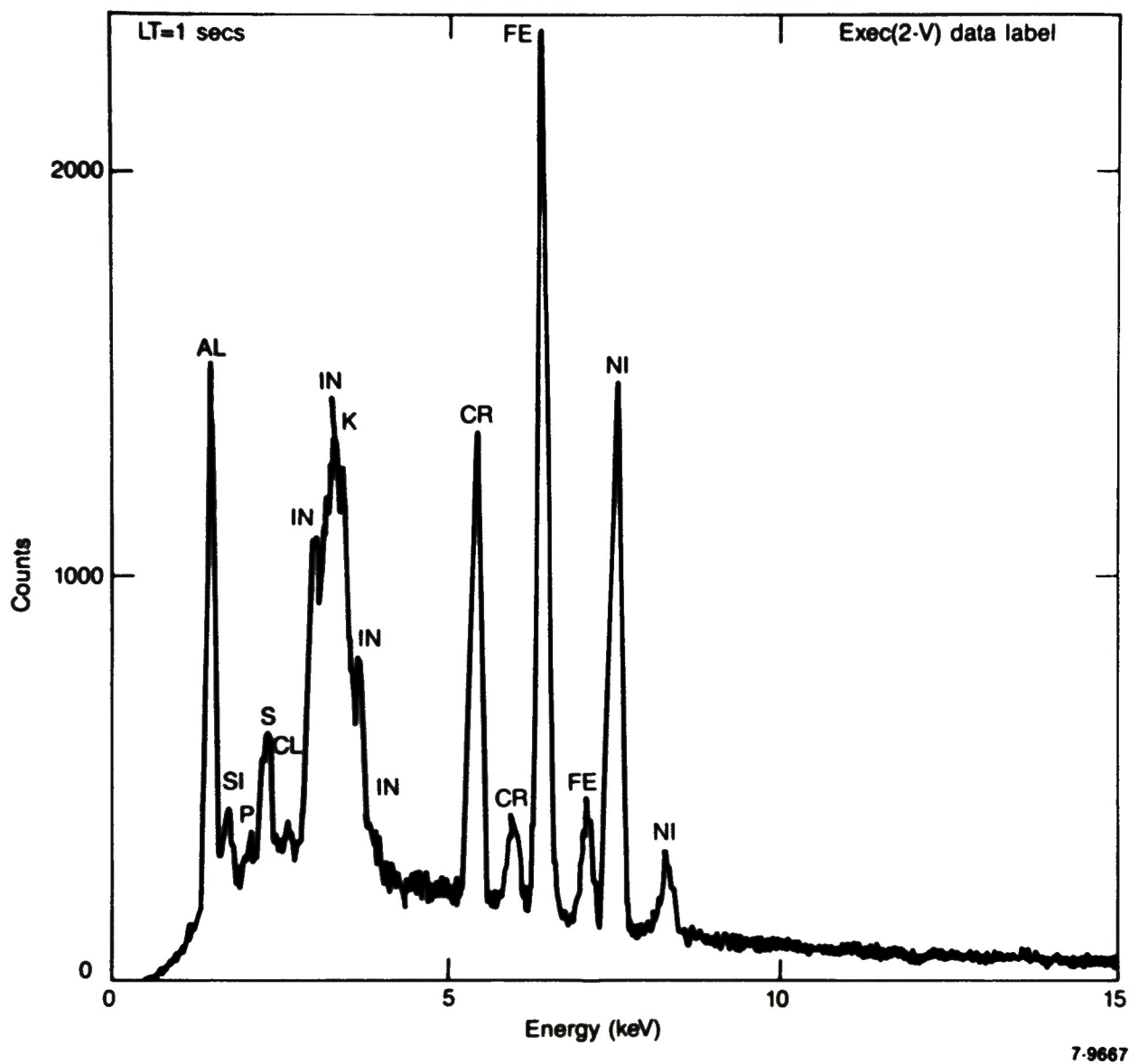


Figure 23c. EDS spectrum of surface deposit from specimen A1.

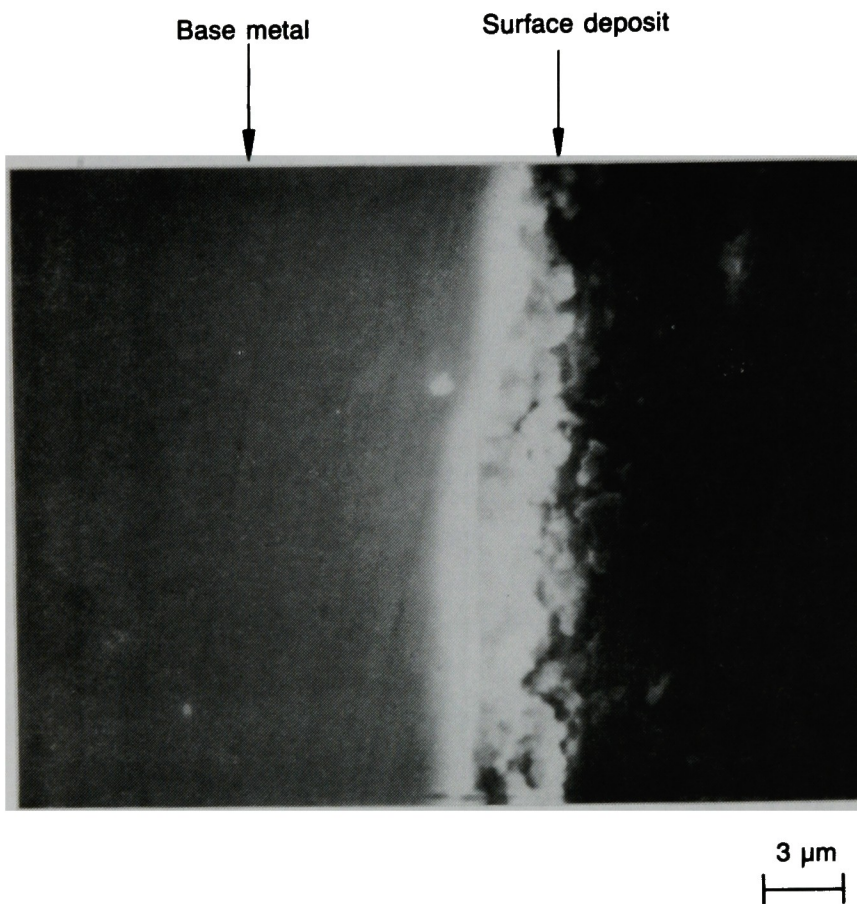


Figure 24a. SEM photograph of specimen B4.

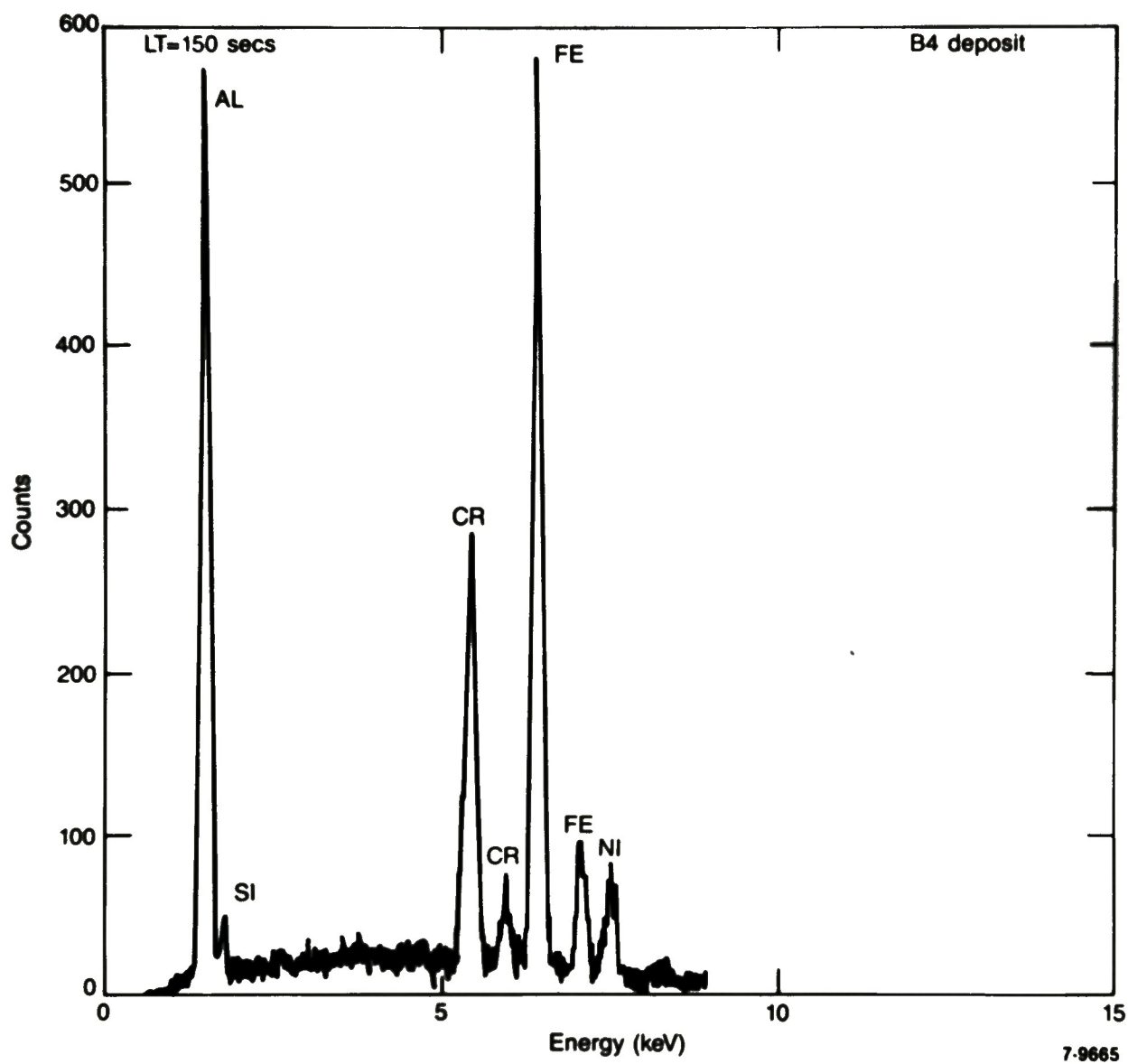


Figure 24b. EDS spectrum of surface deposit from specimen B4.

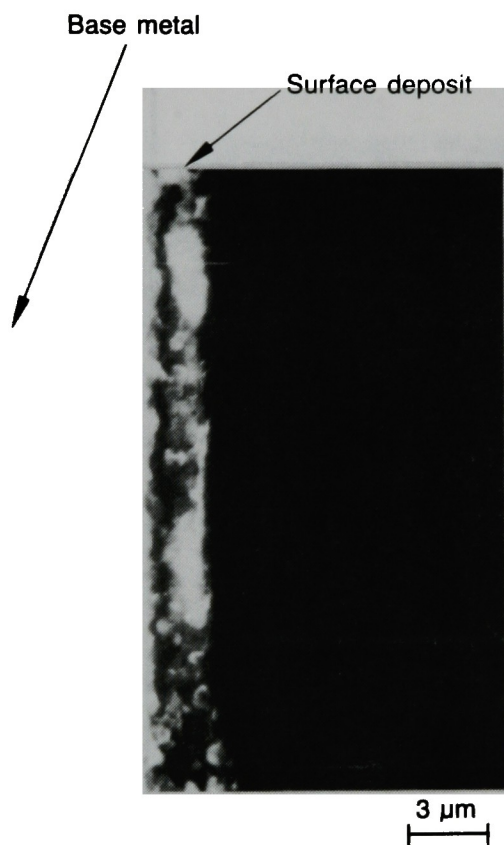


Figure 25a. SEM photograph of specimen P1.

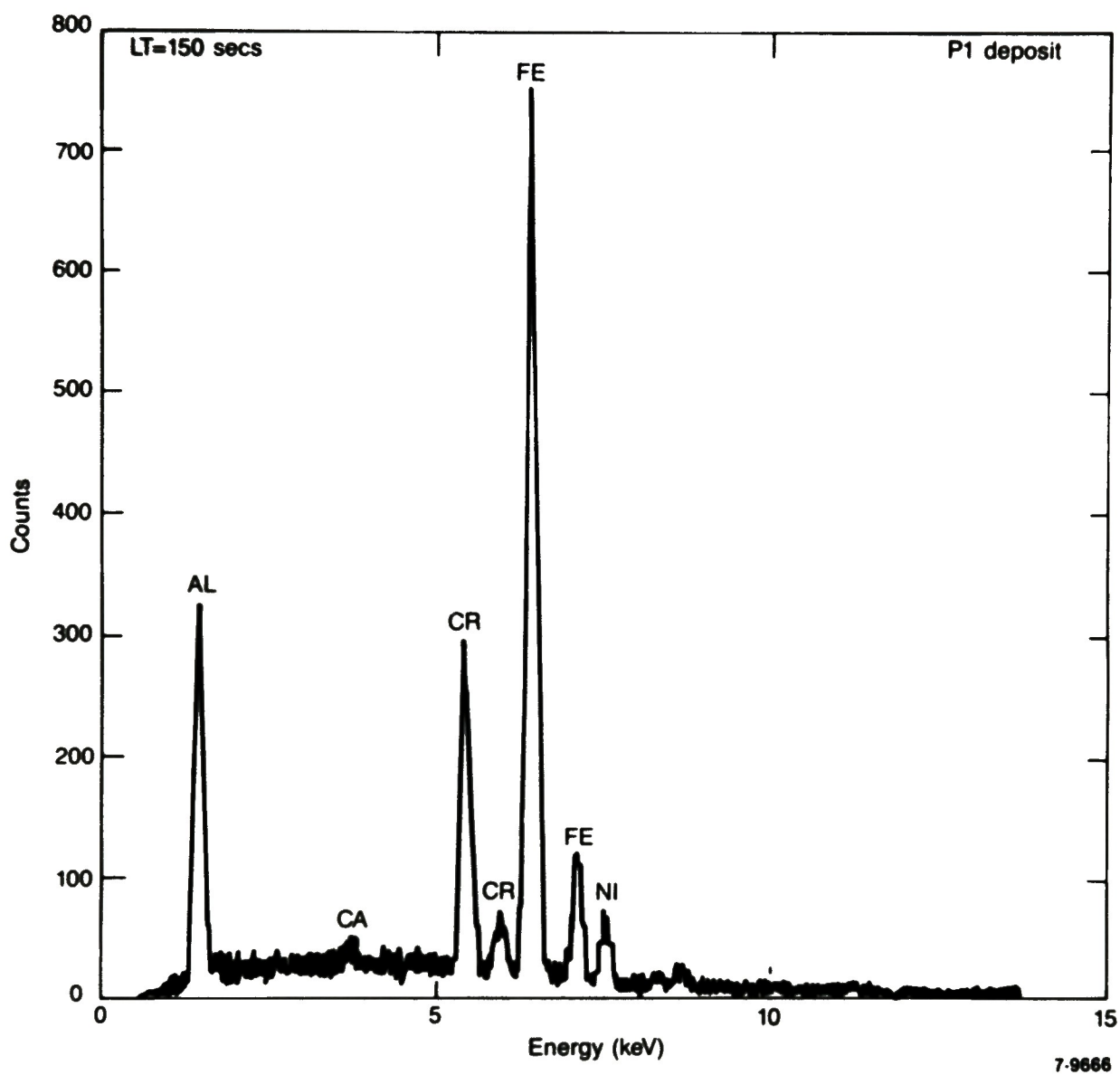


Figure 25b. EDS spectrum of surface deposit from specimen P1.

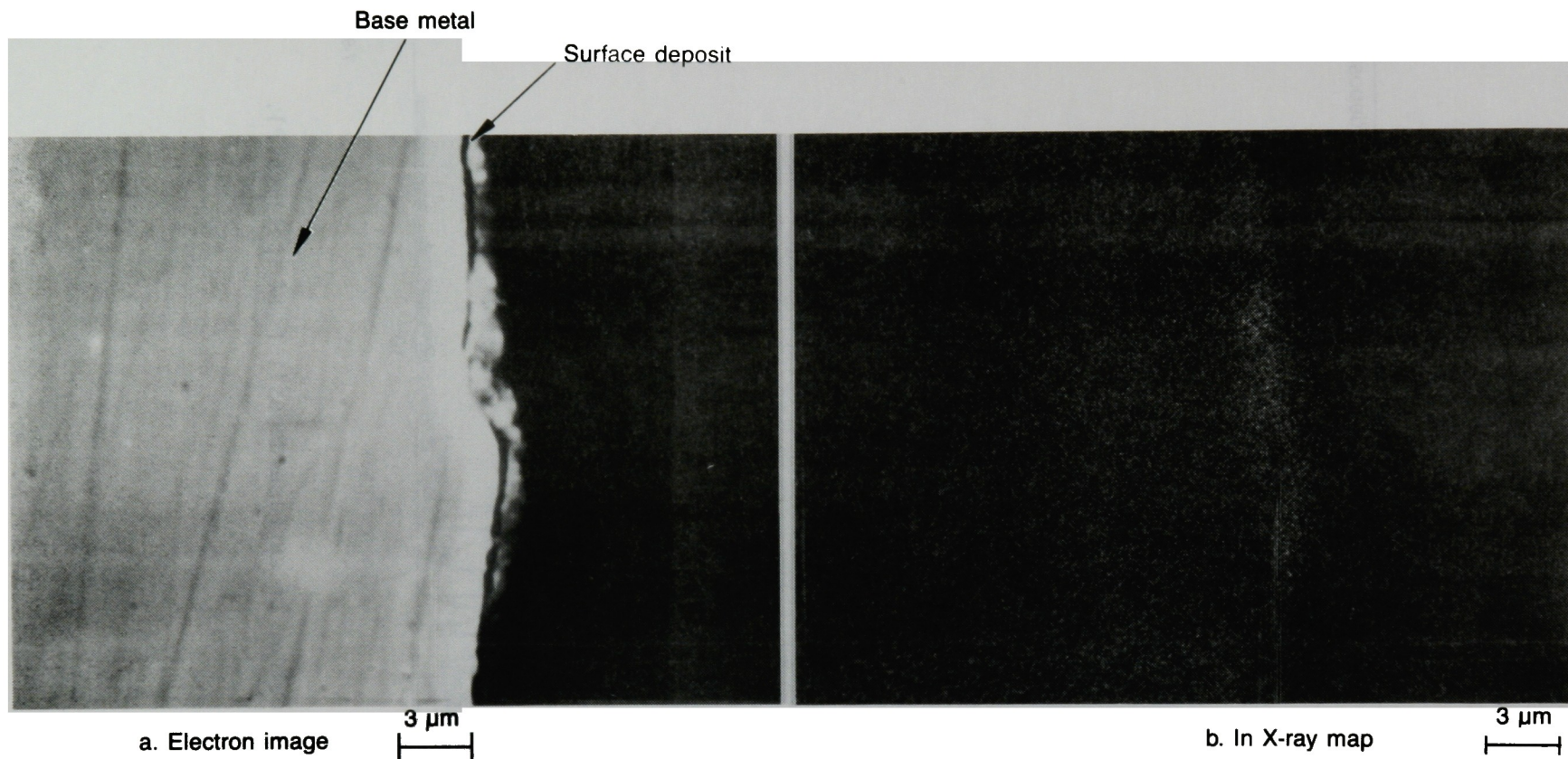


Figure 26a and b. SEM photographs of specimen A4.

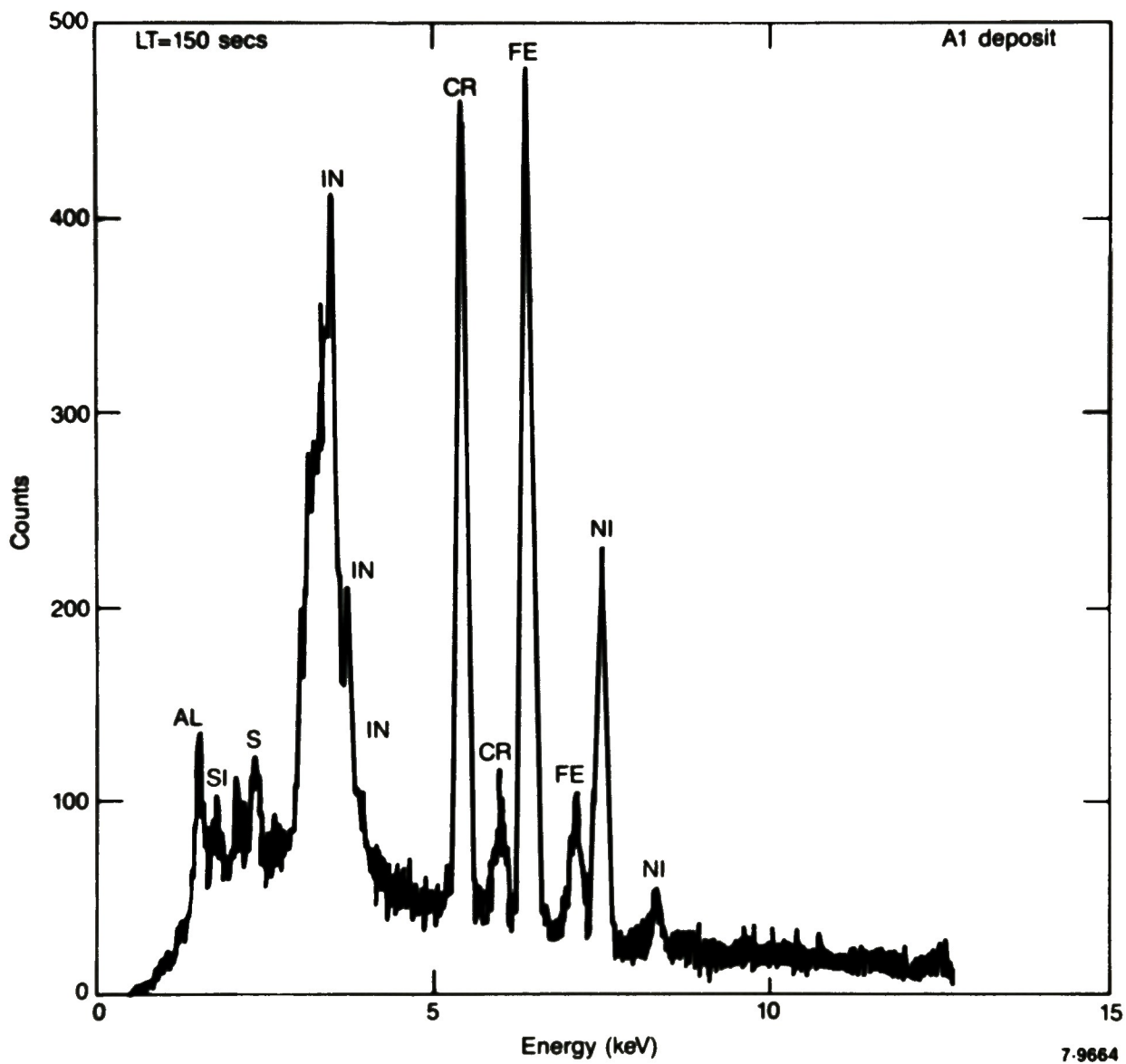
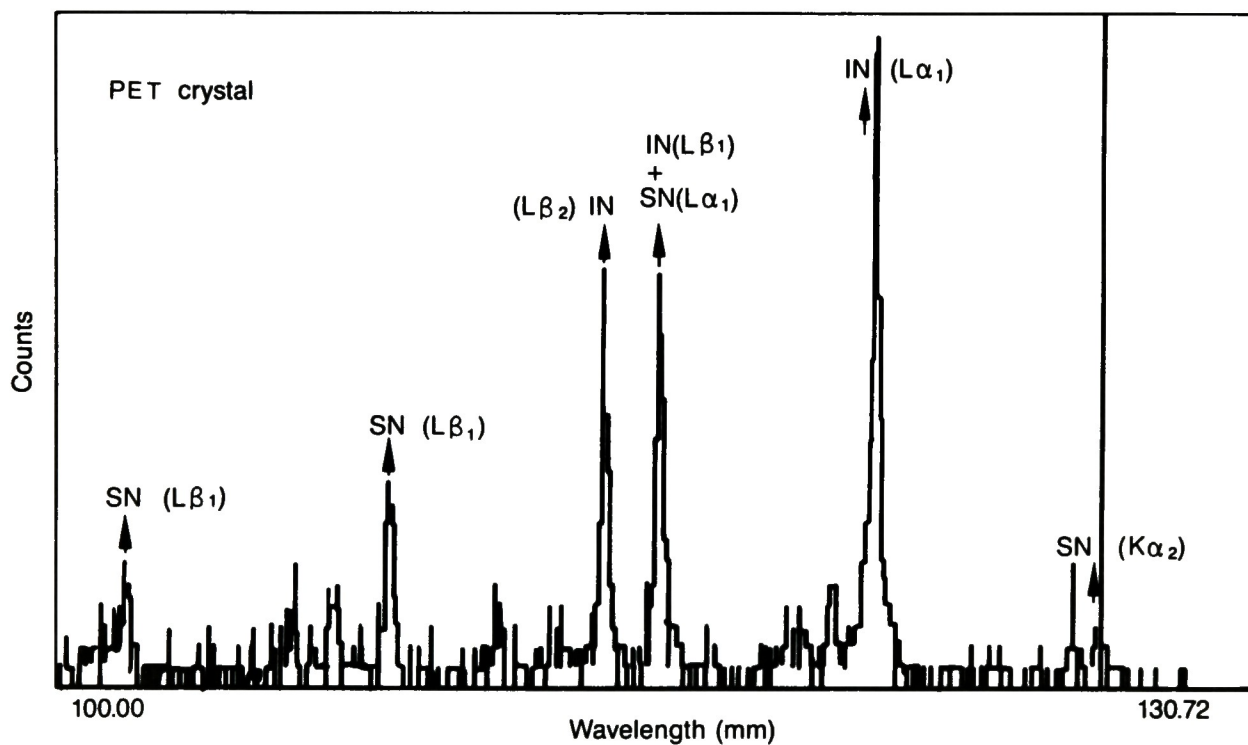


Figure 26c. EDS spectrum of surface deposit from specimen A4.



7-9663

Figure 26d. WDS spectrum of surface deposit from specimen A4.

3. TMI-2 ACCIDENT SCENARIO

The first 16 h of the TMI-2 accident is the period of interest to accident analysis. In particular, from 1 h and 40 min, when reactor coolant pumps 1A and 2A were turned off, until 3 h and 20 min, when high pressure injection was initiated, the core was uncovered for an extended period and underwent heatup, degradation and fission product release. The principal purpose of the examination of the backing plates has been to search for signatures of this period of the accident which could help to better understand the phenomena occurring during the process of severe core degradation. It is recognized that much of the evidence that once existed on these plates has been altered by subsequent events, in particular an extended period of submergence in highly contaminated water.

The steam generator MCB plates were taken from the tops of the A and B steam generators. These regions were probably uncovered throughout the entire time period from 1 h and 40 min until reactor coolant pump 1A was successfully restarted at 15 h and 50 min. During the initial phase of core uncovering, the block valve to the stuck-open pilot-operated relief valve was in the open position and the primary system was depressurizing through the relief line. However, it is unlikely that there was significant release of fission products from the fuel at this time. At 2 h and 20 min, the block valve was closed and remained closed until approximately 3 h and 10 min, shortly before initiation of high pressure injection. During this period, when most of the release of fission products from the fuel is believed to have occurred, there was no loss from the primary coolant system via the pressurizer relief line. Some steam was flowing to each of the steam generators where it was condensed, probably carrying fission product vapors and aerosols with it.

By 3 h, the temperatures at the top of the hot legs had risen to approximately 700 K, where they remained until 10 h. Over much of this time period, the hot legs and steam generators were apparently isolated from the core region. After high pressure injection, the lower portions of the hot legs were apparently filled with water that was subcooled until 11 h. At this time, the A leg temperature dropped to saturation,

indicating the partial reestablishment of steam flow through the hydrogen trapped in the region. The A leg temperature subsequently increased by approximately 310 K, indicating that flow had again stopped. At 15 h and 50 min, water flow was reestablished in both loops.

The pressurizer manway cover is at the very top of the pressurizer. As discussed earlier, the block valve was closed during much of the period of fission product release from the fuel. In addition, the pressurizer contained a substantial quantity of water throughout the accident. Any fission products deposited on the cover plate either passed through the water pool in bubbles, were volatilized from the pool, or were deposited directly from the water while the pressurizer was completely filled. An important event occurred at 2 h and 54 min when the reactor coolant pump 2B was operated briefly. As the core was partially reflooded, the reactor coolant system pressure rose rapidly and a significant quantity of the steam produced by the overheated fuel was condensed in the pressurizer. Fragmented fuel debris, super heated gases, and fission products were probably carried into the pressurizer during this event.

After 3 h and 40 min, the pressurizer remained full of water, except for two periods of approximately 1.5 h duration that occurred at 11 h and 13 h. At 3 h and 45 min, another key event occurred that produced a rapid increase in primary system pressure. The event is believed to be associated with the dumping of molten fuel material into the lower plenum of the vessel. However, it does not appear that much condensation of steam occurred in the pressurizer from this event. The filling rate of the pressurizer is consistent with the rate of introduction of high pressure injection coolant. The rise in cold leg temperatures indicates that much of the steam produced was relieved through the vent valves in the upper plenum to the cold legs.

3.1 Data Evaluation and Analysis

Including Fission Product Inventory Estimation

Table 6 shows the average concentrations of important radioisotopes on Plates A, B, and P as measured in leaching samples at the INEL.⁶ The

TABLE 6. MEASURED SURFACE DEPOSITION AND CORE INVENTORY FRACTIONS OF RADIONUCLIDES DEPOSITED ON THE MCB PLATES

| | Radionuclide Surface Activity ($\mu\text{Ci}/\text{cm}^2$) ^a | | | | | | |
|----------------------------------|--|-----------|-----------|----------|-----------|-----------|----------|
| | Co-60 | Sr-90 | Sb-125 | I-129 | Cs-134 | Cs-137 | Ru-106 |
| Steam Generator A | 7.4 (-2) ^b | 1.8 (-1) | 5.0 (-1) | 7.2 (-6) | 1.6 (-1) | 5.8 (0) | 5.3 (-1) |
| Steam Generator B | 4.4 (-2) | 9.3 (-2) | 2.8 (-2) | -- | 5.5 (-2) | 1.9 (0) | -- |
| Pressurizer | 2.4 (-2) | 4.0 (-1) | 4.3 (-3) | -- | 2.1 (-3) | 4.8 (-2) | -- |
| RTD Thermowell ^c | 1.1 (-1) | 8.9 (0) | 8.3 (-1) | 8.0 (-8) | 4.7 (-1) | 2.0 (1) | -- |
| Implied Total Surface Quantities | | | | | | | |
| RCS Loop Surface | | | | | | | |
| Activity (Ci) | 1.5 (1) | 8.7 (1) | 6.5 (1) | 1.7 (-3) | 2.8 (1) | 1.0 (3) | 1.3 (2) |
| Fraction of Core Inventory | -- | 1.4 (-4) | 3.0 (-3) | 7.4 (-3) | 1.5 (-3) | 1.4 (-3) | 4.6 (-3) |
| Pressurizer Surface | | | | | | | |
| Activity (Ci) | 2.3 (-5) | 3.9 (-4) | 4.2 (-6) | -- | 2.0 (-6) | 4.6 (-5) | -- |
| Fraction of Core Inventory | -- | 6.2 (-10) | 1.9 (-10) | -- | 1.1 (-10) | 6.3 (-11) | -- |

a. Corrected to April 1, 1986.

b. $a(b) = a \times 10^b$.

c. From GEND-057, Reference 7.

activities were decay-corrected to April 1, 1986. These results were reproduced in Table 6. The concentrations measured at the thermowell location are all higher than in the steam generator. Similarly, results tabulated in Reference 7 for the upper plenum surfaces show higher fission product concentrations than in the hot leg.

Using the RTD thermowell data to represent piping and the average of the A and B steam generator values to represent the steam generators, the total surface activity in the primary system loops was calculated. The results are also shown in terms of the fraction of core inventory. It should be noted that the values for primary system surface areas used in Reference 7 are apparently incorrect (steam generator area of $3.7 \times 10^7 \text{ cm}^2$ and piping area of $2.0 \times 10^6 \text{ cm}^2$). Values of $2.4 \times 10^8 \text{ cm}^2$ and $6 \times 10^6 \text{ cm}^2$ were used to represent the steam generator and the piping, respectively, based on analyses performed at TMI-2.⁴ The fractions of the fission product species deposited on the primary system surfaces are all small. This does not imply, however, that the fractions deposited during the accident were small, since deposit of aerosols and soluble species could have been washed away from the surface. The fission product inventory fractions deposited in the pressurizer are extremely small, both because of the small surface available and the low concentration of materials.

At the time that the plates were removed from the plant, gamma activities were measured with a Ge gamma-ray spectrometer.⁴ The values obtained in this manner were typically higher by a factor of 2 to 4 than the values presented in Table 6. The cause of the discrepancy is not clear, although it could be normalization of the spectrometer results. It is also not clear whether any adjustments had been made to the activities reported in Reference 4 or whether they related to the date of the measurement.

There has been some concern expressed that the backing plates from the two steam generators could have been switched in handling. The reasons for the concern arise from an expectation that the B loop surfaces would have higher contamination levels than the A loop because of an extended period

of stagnant conditions in this loop following the accident. Radiation surveys of the loops have indicated a higher contamination level in the B loop, which is consistent with this theory. In addition, there are some inconsistencies between References 3 and 4 with respect to the surface appearance, fuel deposition, and Ce-144 deposition of the plates. The current findings do, however, appear to be consistent with those reported in Reference 4.

The gamma spectroscopic results reported in Reference 4 show the surface activity of the A plate to be higher than that of the B plate, even though the removable activity is lower. Similarly, the thickness of the film on the B plate is reported to be larger than on the A plate both in the previous examination⁴ and the present examination.

Elemental analyses of the material leached from the samples were also performed. For most fission products, the quantities of deposited materials were below detectable limits. Interesting results were obtained, however, for fission product tellurium and the control rod materials, silver and cadmium. Assuming that the deposits on the steam generator backing plates were representative of all of the surface area of the loops, the total mass of tellurium deposited using the ICAP results would be 7 to 10 kg, depending on whether values below the stated limits of detectability represent negligible deposits or the limit values. Since the estimated total core inventory of tellurium is only 3.6 kg, the measured ICAP values cannot be representative of the entire loops. Furthermore, the SSMS results indicate a much lower concentration of tellurium in these samples. The ICAP results do indicate, however, that a significant quantity of tellurium transported a considerable distance before depositing. In state-of-the-art calculations,⁸ the assumed rate of reaction of tellurium with reactor coolant system surfaces is so high that it is predicted to transport only a short distance before reacting with the surfaces or forming an aerosol.

The measured concentration of control rod material, silver, is also very high. Again assuming that the measured concentrations are representative, the total quantity of silver deposited on the loop surfaces

(including steam generator tubes) is 306 kg or 14% of the inventory. In comparison, the cadmium-deposited mass would be 0.87 kg or 0.6% of the inventory. This result is quite different from the ratios of these constituents measured in the core region⁹ and on surfaces in the upper plenum,⁵ in which the mass fractions of silver, indium, and cadmium are similar despite the original composition of 85-15-5. The fact that the least volatile species, silver, appears to have traveled the farthest is undoubtedly a clue to the mode of transport (for example, as an aerosol).

The measured ratios of some isotopes also provide interesting results. The ratios of the 134 to 137 isotopes of cesium are 0.052 and 0.055 for the A and B steam generators and 0.084 for the pressurizer, indicating that the pressurizer cesium originated from a region of higher burnup. In contrast, the plutonium concentration in fuel on the pressurizer surface was lower than on the steam generator surfaces,⁴ indicating that the fuel in the pressurizer came from a region of lower burnup. A possible explanation is that the deposition in the pressurizer resulted from material transported at the time of reactor coolant pump operation at 2 h and 54 min. The cesium (probably as CsOH) transported with the steam into the pressurizer was from the hottest, high burnup region of the core, whereas the fuel carried into the pressurizer came from the fragmentation of lower burnup fuel at the top of the core.

3.2 Interpretation of the Results

The amounts of fission products measured in the steam generator and pressurizer represent small fractions of the fission products released from the fuel during the accident, with the possible exception of tellurium deposition. Considering the long time period of submersion following the accident, the small values observed for most of the fission products are not at all surprising. Interesting results were obtained for the measured quantities of tellurium and silver. In each case, the potentially large quantity of deposited material has implications regarding the form of material transport. Although some possible explanations have been offered, it would be speculative to draw conclusions at this time.

4. REFERENCES

1. M. L. Russell et al., TMI-2 Accident Evaluation Program Sample Acquisition and Examination Plan--Executive Summary, EG&G-TMI-7121, EG&G Idaho, Inc., December 1985.
2. E. L. Tolman et al., TMI-2 Accident Evaluation Program, EGG-TMI-7048, EG&G Idaho, Inc., February 1986.
3. M. Lambert, Alpha Measurements and Surface Scrape Samples of the Pressurizer Manway Diaphragm, TB 86-16 Rev.0, GPU Nuclear Corp., March 13, 1986.
4. J. Greenborg, Deposition of Fuel on the Inside Surfaces of the RCS, TMI-2 Technical Bulletin TB 86-37, September 4, 1986.
5. M. P. Failey et al., The Examination of the Leadscrew Support Tube from Three Mile Island Reactor Unit 2, GEND-INF-067, March 1986.
6. Letter report from R. Simmons to B. Saffell, Steam Generator Manway Backing Plate Examinations, January 26, 1987.
7. S. Langer et al., TMI-2 Fission Product Inventory Program FY-85 Status Report, GEND-057, November 1986.
8. J. A. Gieseke et al., Source Term Code Package: A User's Guide (Mod 1), NUREG/CR-4587, July 1986.
9. D. W. Akers et al., TMI-2 Core Debris Grab Samples--Examination and Analysis, Part I, GEND-INF-075, September 1986.

